FFI RAPPORT

MATCHED-FIELD LOCALIZATION OF EXPLOSIVE SOURCES IN THE BARENTS SEA USING A HORIZONTAL ARRAY

TOLLEFSEN Dag

FFI/RAPPORT-2002/04480

FFIBM/786/115

Approved
Horten 25 November 2002

J K Johnsen
Director of Research

MATCHED-FIELD LOCALIZATION OF EXPLOSIVE SOURCES IN THE BARENTS SEA USING A HORIZONTAL ARRAY

TOLLEFSEN Dag

FFI/RAPPORT-2002/04480

FORSVARETS FORSKNINGSINSTITUTT
Norwegian Defence Research Establishment
P O Box 25, NO-2027 Kjeller, Norway

FORSVARETS FORSKNINGSINSTITUTT (FFI)
Norwegian Defence Research Establishment

P O BOX 25
N0-2027 KJELLER, NORWAY

UNCLASSIFIED

SECURITY CLASSIFICATION OF THIS PAGE
(when data entered)

REPORT DOCUMENTATION PAGE

1) PUBL/REPORT NUMBER	2) SECURITY CLASSIFICATION	3) NUMBER OF PAGES
FFI/RAPPORT-2002/04480	UNCLASSIFIED	47
1a) PROJECT REFERENCE	**2a) DECLASSIFICATION/DOWNGRADING SCHEDULE**	
FFIBM/786/115	-	

4) TITLE

MATCHED-FIELD LOCALIZATION OF EXPLOSIVE SOURCES IN THE BARENTS SEA USING A HORIZONTAL ARRAY

5) NAMES OF AUTHOR(S) IN FULL (surname first)

TOLLEFSEN Dag

6) DISTRIBUTION STATEMENT

Approved for public release. Distribution unlimited. (Offentlig tilgjengelig)

7) INDEXING TERMS

IN ENGLISH:	IN NORWEGIAN:
a) Underwater Acoustics	a) Undervannsakustikk
b) Signal Processing	b) Signalbehandling
c) Matched Field Processing	c) Medietilpasset signalbehandling
d) Source Localization	d) Kildelokalisering
e)	e)

THESAURUS REFERENCE:

8) ABSTRACT

Matched-field processing (MFP) techniques are used to estimate the range and depth of underwater explosive sources. Data from an experiment conducted by FFI in the Barents Sea 1999 is used. The experiment was conducted in a relatively flat area, using explosive (SUS) sources and a 31-element receiver array. Low-frequency data from shots endfire to the ten-element bottom mounted horizontal section of the array (length 820 m) is used in this report.

A two-step method is employed. The first step (environment focusing) makes use of data from known sources in matched-field inversion for the estimation of seabed geoacoustic model parameters. The second step (source localization) employs use of the incoherent broadband Bartlett processor and a fast normal mode acoustic propagation model (C-SNAP) in an exhaustive search for source range and depth in the model environment obtained in the first step. The second step is fast, requiring less than a minute of computer time on a 1.1 GHz processor. Excellent results are obtained when combining data from two 10 Hz wide frequency bands centred at 40 Hz and within 80-110 Hz, with source positions determined to within 200 m in range and 6 m in depth for ten sources at ranges 3-27 km from the array.

9) DATE	AUTHORIZED BY	POSITION
	This page only	
25 November 2002	J K Johnsen	Director of Research

ISBN 82-464-0665-5

UNCLASSIFIED

SECURITY CLASSIFICATION OF THIS PAGE
(when data entered)

CONTENTS

MATCHED-FIELD LOCALIZATION OF EXPLOSIVE SOURCES IN THE BARENTS SEA USING A HORIZONTAL ARRAY[1]

1 INTRODUCTION

The localization of underwater sources in shallow water using a single acoustic array can be a complicated task. The received signal will be distorted due to multipath propagation and can often not be analysed using a conventional plane-wave description. Moreover, conventional methods will provide a bearing estimate, possibly a range estimate, and rarely a source depth estimate. To overcome these limitations, an alternative signal processing method, matched-field processing (MFP) (1), has been developed and applied to underwater acoustic problems over the last fifteen or so years. Localization of sources in range, depth and bearing by application of MFP has been demonstrated for deep and shallow water environments (2,3,4).

To test matched-field processing methods, an acoustic experiment was conducted by FFI in the Barents Sea in August of 1999 (18). The experiment used broadband explosive sources and a 31-element receiving acoustic array deployed in a combined vertical-horizontal configuration. Previous analysis of this data has included matched-field inversion for estimation of seabed parameters and localization of sources using vertical array data (21,22). The present report applies matched-field techniques to localization of sources at short to moderate ranges using data recorded at the 10-element bottom mounted horizontal array.

This report is organized as follows: a short outline of matched-field techniques as used in this report is provided in chapter 2. The acoustic experiment and data is described in chapter 3. Results from matched-field inversion for seabed properties are demonstrated in chapter 4 and for source localization in chapter 5. Chapter 6 discusses the results and outlines possible extensions of the present work. Some additional results are confined to the Appendix.

2 METHODS

Matched-field processing has been successfully applied to localization of sources in deep and shallow water. Chapman and McKirdy (6) located a SUS charge at range 18 km in deep water matching low-frequency data recorded at a vertical array. Jesus (7) applied broadband processing to 250 Hz data recorded at a vertical array in shallow water (depth 120 m) at ranges to 20 km. Brienzo and Hodgkiss (8) applied waveform matching to shot data at 1-100 Hz recorded on a vertical array at range 9 km in deep water. Gerstoft and Gingras (10) used multi-frequency data in bands centred at 170 Hz and 330 Hz recorded at a vertical array at range 6 km in shallow water. Matched-field techniques for application to inversion for environment parameters (13) and to the estimation of environment and source parameters in a

[1] Work presented at the OCEANS conference, 29-31 October 2002, Biloxi, USA.

combined approach (5) have subsequently been developed and demonstrated. Source localization and inversion for seabed properties is described in brief as separate processes in the following.

2.1 Source localization

2.1.1 The acoustic field and array

Matched-field processing (MFP) as applied in this report requires the acoustic field to be measured over a series of hydrophones of an acoustic array of some aperture, but requires no a priori knowledge of the source (spectrum or levels) in itself. MFP can in principle be applied to an acoustic array in any configuration. In practice, many applications have been demonstrated using vertical arrays (VLA) (6,7,8,10) while applications using horizontal arrays (HLA) seem as yet not to have been explored to the same extent. Notable exceptions using a HLA are Ozard (4) and the SWellEX series of experiments (see references in (11)). Some virtues of a VLA are their relative ease of deployment, their ability to discriminate sources in depth and their finite length limited by the water depth. Some limitations are their inherent inability to determine source bearing and susceptibility to system noise and shape distortions due to array movement induced by water currents. Some virtues of a bottom mounted HLA are their operative advantages, stable configuration once deployed and lower system noise; a limitation is in general a larger aperture requirement.

2.1.2 The Bartlett processor

In essence, matched-field processing is a spatial correlation process where a pressure field measured over an acoustic array is correlated with a synthetic or replica field computed for a set of trial positions in a model environment.

Correlation can be measured using the classical Bartlett processor

$$B(x) = q^{+}(x, m, \omega_k) R(\omega_k) q(x, m, \omega_k) \tag{2.1}$$

with $q(x,m)$ the modelled acoustic field at trial position x in model environment m.

$$R = \left\langle pp^{+} \right\rangle \tag{2.2}$$

is the data covariance matrix constructed from the measured complex acoustic pressure field p, all terms at frequency component ω and normalized to unity. The virtue of using normalized pressure is that knowledge of the source waveform or spectrum is not required. This suits the application to SUS explosive charges, which are not well calibrated at single frequency components. In expanded form, the Bartlett processor takes the form:

$$B(x) = \frac{\left|\sum_{j=1}^{N} p_j^{+} q_j(x,m)\right|^2}{\sum_{j=1}^{N}\left|p_j\right|^2 \sum_{j=1}^{N}\left|q_j(x,m)\right|^2} \tag{2.3}$$

with j a summation index over N hydrophones, the frequency index omitted. The processor takes on a maximum value of one for perfect match and a value of zero for no match.

When applied to data at multiple frequencies (3) the processor expands to:

$$B(x) = \frac{1}{M}\sum_{k=1}^{M}\left[\frac{\left|\sum_{j=1}^{N} p_{jk}^{+} q_{jk}(x,m)\right|^2}{\sum_{j=1}^{N}\left|p_{jk}\right|^2 \sum_{j=1}^{N}\left|q_{jk}(x,m)\right|^2}\right] \tag{2.4}$$

with k a summation index over M frequency components. This is recognized as an incoherent sum over single-frequency Bartlett processors (2.3) using the same weight to all components. This will be referred to as the broadband incoherent Bartlett processor.

For completeness, a definition of Bartlett *energy* is also used. Here the definition

$$E_B = 10\log(B(x)) \tag{2.5}$$

with $B(x)$ the Bartlett processor of (2.3) or (2.4) will be used. The maximum Bartlett energy is then 0 dB for perfect match, decreasing to negative values for less than perfect match.

The Bartlett processor was proposed at the early stages of MFP development and remains popular due to its simplicity and often-remarkable robustness. Variants of the broadband processor, most of these assuming additional knowledge of the source properties have subsequently been proposed, but will not be considered in this report.

2.1.3 The replica field

The replica field in (2.4) is computed using a numerical acoustic propagation model. Issues to consider in the choice of model are required level of complexity in description of the environment, the acoustic field quantities desired as output and required speed in computation. For the present work, the normal mode C-SNAP (17) was chosen for its speed and sufficient accuracy in treating the seabed environment at the site. The model solves for the complex pressure field in a range-independent two-layer fluid seabed environment using a normal mode decomposition of the field.

The normal mode sum formulation for the pressure field is given by (e.g. 15, Eq. 5.13):

$$p(r,z) \cong \frac{i}{\sqrt{8\pi r}} e^{-i\pi/4} \sum_{m=1}^{M} \Psi_m(z_S)\Psi_m(z)\frac{e^{ik_{rm}r}}{\sqrt{k_{rm}}} \tag{2.6}$$

with $\psi(z)$ the mode functions, z_S and z the source and receiver depth, r the source range, k_{rm} the horizontal wavenumbers, m a mode index and M the number of modes.

A virtue of using a normal mode code is that mode functions need only be computed once (per frequency) for a given environment. The synthetic field at trial positions is then easily computed by inserting the trial range and depth in the expression for the acoustic field (the variables r and z in Eq. 2.6). This reduces the computation time considerably over e.g. a wavenumber integration type or a parabolic equation type model where the wave equation has to be solved for every trial source depth of the problem.

In searching for source range and depth, an exhaustive search over all trial positions is performed. Search intervals and increments are set up in range and depth, with the value of the Bartlett function computed at each grid point; the resulting matrix termed the ambiguity surface. The position yielding the maximum value of the Bartlett function is taken to be the estimated source position. This method was adopted by Fizell (2) at the early development of MFP. The replica fields are computed for a fixed model environment, whether perfectly known as would be in a simulation study, based on input from existing environment databases, or otherwise known to a best model approximation for the application at hand. The procedure adopted in the present work is outlined in the next section.

2.2 Environment focusing

In the present work, an initial environment model is set up based on available geophysical information (a bathymetry profile and a seismic profile). Model parameters are then estimated by matched-field inversion of acoustic data. At the outset, a range-independent environment model consisting of a water layer and a seabed of some complexity is set up. The model is then refined or reduced until a suitable description of the true environment at the actual experiment site and for the application is obtained. Some simplifying assumptions in the environmental model as used in this work are:

- uniform water depth,
- two homogeneous seabed layers,
- each seabed layer described as a *fluid* medium by three parameters: compressional (p-) wave velocity, p-wave attenuation and density,
- a single sound speed profile in the water column.

The environment model is depicted in Figure 2.1. Previous work not reported further herein has shown that this simplified model provides a reasonable description for the present application and for this experiment site.

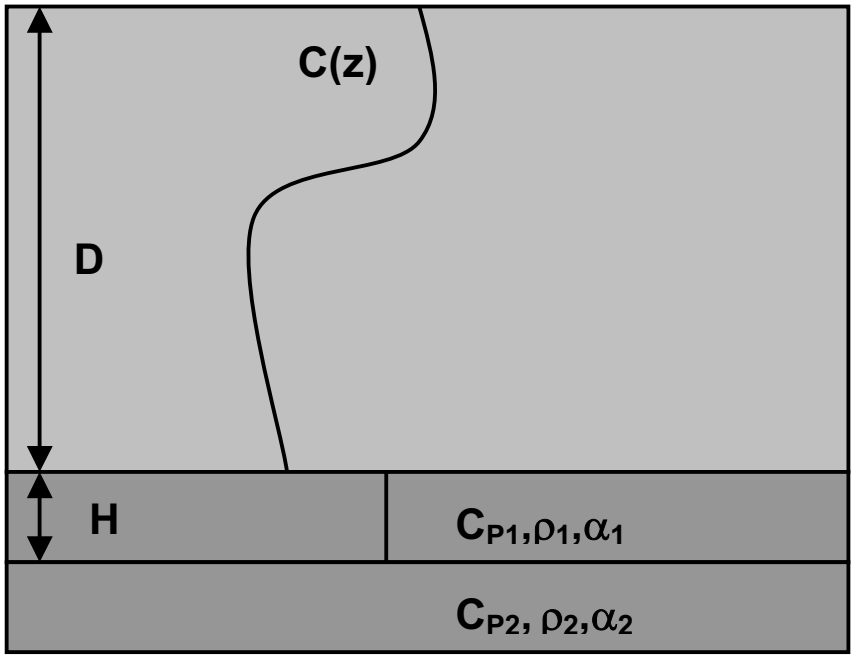

Figure 2.1 Simplified environment model consisting of a water layer (sound speed profile c(z), water depth D) over a two-layer fluid seabed (seven seabed parameters indicated).

Matched-field inversion is essentially an extension of the correlation process of (2.1), now with the set of environmental parameters m unknown and source position x fixed to a priori known values. Candidate models are typically searched over in an optimisation process (energy E(m)=1-B(m) minimized) until an acceptable match model has been found. For a range-independent two-layer fluid seabed model as described above, there are in principle seven unknown seabed parameters (three each in two layers plus the sediment thickness). Available a priori information from the area of experiment may help fix one or a few of these parameters, but even so the possible total number of combinations of parameters is potentially large (e.g. 10^{14} if each parameter is assigned one hundred equally probable values). Since the wave equation in principle has to be solved for each set of trial environment parameters, this in practice precludes the use of an exhaustive search over candidate models. Much effort in current research has been directed towards the development of effective search methods in inversion of acoustic data for geoacoustic properties of the seabed (13). Two efficient global search techniques have gained widespread use for problems of this nature: simulated annealing and genetic algorithms. For the present work, the genetic algorithm global search method of SAGA (9) has been used. SAGA performs a non-exhaustive global search through the parameter space towards an optimal (best-match) model using a genetic algorithm method. The final model or *inversion model* is in the present work taken to be the collection of parameter values yielding the maximum of the posterior probability distributions per model parameter. These distributions are approximations to the true probability distributions (which would require integrating over all possible models), in SAGA computed by integrating over a subset of the models collected in the search process.

There are several limitations to the matched-field inversion approach used herein. First are the assumptions of the environment model: range independence and two homogeneous fluid seabed layers. Neither may approximate the true environment well. Second is the choice of acoustic data used in the correlation process: only a subset of available data (here: a small number of frequency components) is used. Moreover, the global search method may converge toward a "false" optimal model. These sources of error are noted but are not particular to the present application of matched-field methods (14).

2.3 A two-step approach

The two-step method as used in this report consists of:

- Environment focusing - inversion for seabed parameters using a range-independent environment model. Multi-frequency shot data is used. This step establishes an optimal seabed model for the area of experiment.
- Source localization - exhaustive search for source position in range and depth using the environmental model obtained in the first step. Multi-frequency or broadband data is used, within the same span of frequencies as first step.

Results using this two-step approach are presented in chapter four and five. The steps are combined into a single optimisation procedure in appendix C. Note that for the present work, some sources were used in both steps, though with a different set of frequency components selected for use in each step.

2.4 Bathymetry representation

The ambiguity surfaces in the second step are computed using the forward model C-SNAP in a range-independent mode. This requires selecting or determining a water depth for the acoustic field computations. Some evident choices are the water depth measured at the array site, the depth measured at a trial range, or water depth as input from other a priori information such as a bathymetry database. For the approach adopted in this report, a priori information of bathymetry along the acoustic track is available, and an equivalent representation of the true bathymetry is used, eliminating the need to resort to use of a fully range-dependent forward model. The intention is to reduce total computation efforts.

Zakarauskas et al (12) presented a derivation of the equivalent or effective water depth approximation to a range-dependent bathymetry. The basic idea is to replace a true range-dependent bathymetry profile with a model profile or a single water depth providing an *equivalent* effect on the acoustic field measured at the receivers. The localization problem is then augmented to determine a set of parameters

$$\mathsf{m} = \{z_S, r_S, d_1, d_2, \ldots, d_N\} \tag{2.7}$$

with the first two parameters the source depth and range and the remaining a set of effective water depths at a chosen number of N segments in range. The concept applies to situations of weakly range-dependent bathymetry and has been applied to single-frequency cases.

In one approach, the set of effective water depths can be included as search parameters in a global optimisation process, the search bounds limited by available a priori information available (e.g. from a database) or a crude assessment of maximum and minimum depth in the area of interest. For a better known or measured bathymetry profile, an analytic expression for the equivalent bathymetry profile can be used.

The optimal equivalent or "effective" water depth is given by (12):

$$D_{eff} \equiv \left(\overline{d^{-2}} \right)^{-1/2} \tag{2.8}$$

where the expression within brackets is

$$\overline{d^{-2}} \equiv \frac{1}{r_S} \int_0^{r_S} \frac{dr}{d^2(r)} \tag{2.9}$$

with r_S the source range and $d(r)$ the true bathymetry profile. The integral can be approximated by use of a trapezoidal rule. For a constant-slope bathymetry the expression reduces to:

$$D_{eff} = \sqrt{d_0 \cdot d(r_S)} \tag{2.10}$$

with d_0 the water depth at the array and $d(r_S)$ the water depth at the source range.

The expression (2.9) can also be interpreted to mean that there exists an acoustically equivalent flat bathymetry yielding the same effect on the acoustic field as would a fully range-dependent description. This bathymetry will be denoted the *equivalent water depth*. This interpretation is adopted herein. This makes possible use of a range independent forward model for the acoustic field computations. The ambiguity surfaces are computed using the C-SNAP forward model in range-independent mode.

To summarize, for a known bathymetry profile, an equivalent depth can be computed at each range step of the ambiguity surface, thus the *bathymetry-optimised* ambiguity surface (12) can be readily computed using a range-independent forward model. This approach will be pursued in chapter 5. For a bathymetry not precisely known, the method entails assessing the shallowest and deepest possible effective bathymetries from (2.8), then use a search for an optimal equivalent bathymetry profile in an optimisation process. This approach is termed *bathymetry focalization* and will be pursued in Appendix C.

3 THE ACOUSTIC EXPERIMENT

An acoustic experiment was conducted in the Barents Sea in August of 1999 (18). The experiment was designed to test matched-field processing techniques in a shallow water area. It made use of broadband explosives (SUS) sources and a 31-element acoustic array deployed in a combined vertical-horizontal configuration. Two ships were in use: the R/V H U SVERDRUP II was anchored close to the receiver array while sources were deployed from KV POLARVAKT in three radial runs, in each direction to maximum ranges of 100-120 km from the array. The experiment is depicted in Figure 3.1.

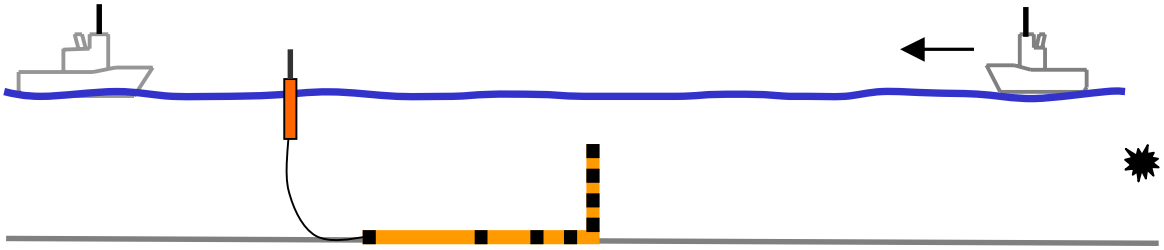

Figure 3.1 *Sketch of the Barents Sea 1999 experiment. A 31-element acoustic array was deployed in a combined vertical-horizontal configuration. The ship R/V HU SVERDRUP II was anchored closed to the receiver position. The source ship KV POLARVAKT deployed explosive sources endfire to the horizontal array.*

Supporting geophysical measurements consisted of a bathymetry profile using a SIMRAD EA-500 echo sounder, a seismic reflection profile along the acoustic track, a number of seismic refraction velocity measurements, and sediment profiles from SIMRAD TOPAS PS018 bottom-penetrating sonar. These supporting measurements, except for the sound speed profile measurements in water, were recorded by R/V H U SVERDRUP II a few days after the collection of acoustic data. Standard analysis of collected geophysical data has produced *baseline* geoacoustic models for the acoustic tracks (20). The environment along the track considered in this report, consisting of a Quaternary sediment layer of estimated thickness 20-40 m over Tertiary sediment, can be characterized as relatively benign.

A bathymetry profile for the portion of the eastward and westward tracks analysed in this report is shown in Figure 3.2. It is noted that the bathymetry is slightly sloping, with a near-constant slope from about 280 m water depth (30 km westward) to about 340 m (8 km eastward). The average slope is 0.10 deg.

Shots at nominal ranges 3-27 km in the westward direction and 3-8 km in the eastward direction were selected for analysis in this report. The shots, nominal ranges (as determined from GPS positions), nominal source depths (as determined by analysis of the bubble pulses of each shot individually) and the water depth at the shot detonation site (as recorded with an EA-500 echo-sounder) are listed in Table 3.1. Seven of the shots were shallow, detonated at approximately 18 m; five of the shots were deep, detonated at approximately 90 m.

Shot Label	Source Type	Source Range [km]	Source Depth [m]	Water Depth [m]	Use
E109 S	Mk-61	8.70	17.3	342.8	I L
E110 D	Mk-82	7.76	86.2	338.3	L
E115 S	Mk-61	3.18	17.2	325.5	I L
W141SM	Mk-64	-3.47	18.3	313.5	I
W139SM	Mk-64	-4.05	17.2	310.7	L
W127 S	Mk-61	-8.07	17.1	303.0	I L
W125 D	Mk-82	-9.79	88.5	296.3	L
W122 D	Mk-82	-11.52	85.6	297.3	L
W121 S	Mk-61	-13.12	18.9	292.8	I
W116 D	Mk-82	-17.37	98.6	286.5	L
W112 S	Mk-61	-19.10	17.7	284.3	L
W104 D	Mk-82	-27.28	82.8	277.3	L

Table 3.1 *Sources (SUS charges) selected for analysis in this report. Ranges are positive eastward from the position of the vertical array. Water depth is as recorded by an EA-500 echo sounder during a bathymetry survey [corrected by -5.0 m from reported values]. Source range and depth are nominal. The letters in column six indicate inversion "I" and source localization "L".*

Data from 31 hydrophones of the array was digitised at 3 kHz. Time segments of length 5.0 sec were selected for processing from each shot. A 65k FFT was applied to the unfiltered time segments, yielding a frequency bin width of about 0.2 Hz. Individual frequency components were selected within peaks of the spectra. For each selected frequency component, the complex pressure vector was stored to a file for further use.

Due to a difference in preamplifier gain on seven of the hydrophones of the horizontal array (where the gain was +12 dB higher) signals received on these phones were substantially saturated or "clipped" for short-range shots. This is especially so for all Mk-64 shots. The occurrence and level of spurious and intermittent noise on these hydrophones was found to be low, as assessed by manual inspection of the recorded time-series. The signal-to-noise ratio per phone has been estimated using the sonar equation to be on the order of 30-40 dB at the ranges of interest for a frequency of 100 Hz. An ambient noise level of 78 dB is then used to account for the proximity of the receiving ship. The actual noise levels have not been estimated from data.

The horizontal array had 10 elements of nominal spacing increasing from 20 m to 240 m, with a total length of 819 m. An array calibration run was performed after deployment. Small explosives charges were dropped in a circle (radius 2 km) around the array. The array orientation was estimated using measured travel times (assuming a straight-line shape with nominal element spacing and a fixed sound speed in water) of these charges (19).

.

Oceanographic profiles (sound speed profile at the receiver position using a CTD cast and temperature profiles at the source ship using XBT casts) were taken intermittently. Figure 3.3 provides profiles taken during the part of the experiment considered in this report.

Weather conditions were relatively severe during the period of the collection of the acoustic data, with 10-15 m/s winds and sea state 4-5 and 3 during the eastward and westward runs respectively. Weather was rougher between the two acoustic runs. The data considered in this report was collected during 1-2 hour periods approximately 40 hrs apart.

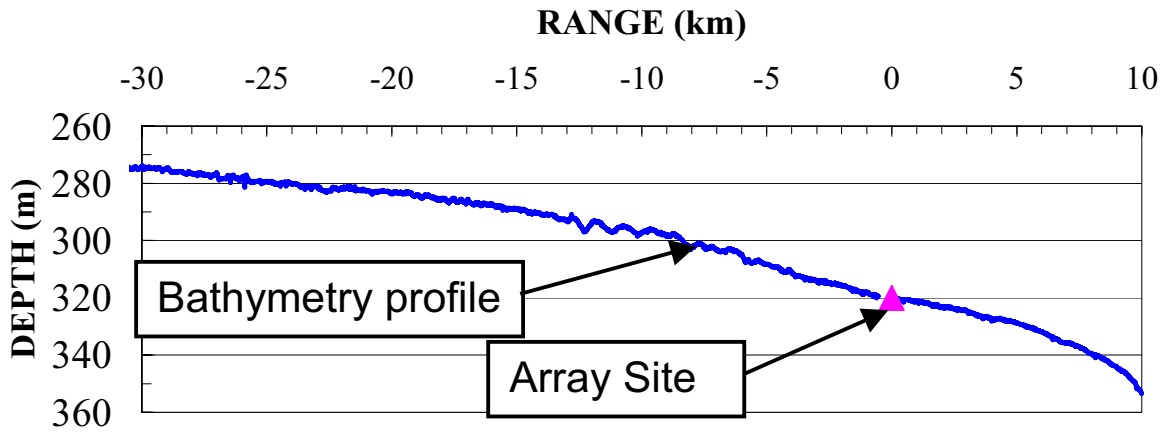

Figure 3.2 *Bathymetry profile. The triangle indicates the position of the vertical array. Range (in km) is negative westward.*

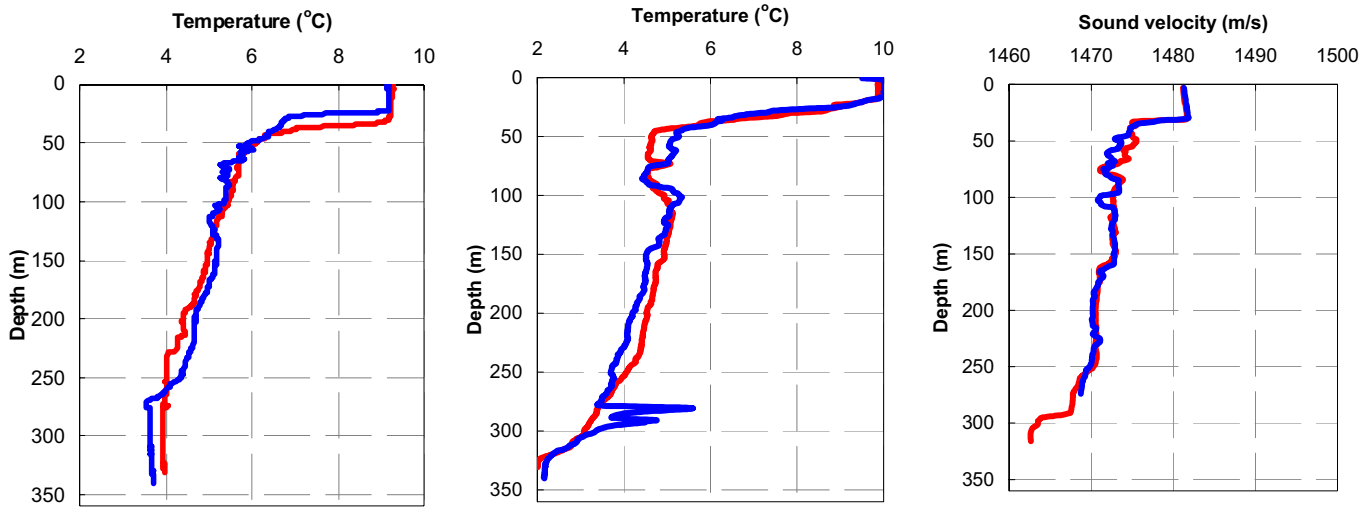

Figure 3.3 *Oceanographic profiles. Temperature profiles measured at source ship during eastward (left panel) and westward run (middle panel) and sound velocity profiles measured at receiver ship during westward (right panel, blue line) and eastward (right panel, red line) runs.*

4 ENVIRONMENT FOCUSING

4.1 Selection of data

Five shallow shots marked with an "I" in the last column of Table 3.1 were used in the inversion step. Five frequency components over the interval 40-140 Hz were selected at spectral peaks (for shallow Mk-61 shots: 40.4 Hz, 57.9 Hz, 80.7 Hz, 96.1 Hz and 128.7 Hz). All inversions were done using data from the 10 elements of the horizontal array. The multi-frequency incoherent Bartlett processor was applied in all cases. Independent inversions were performed using the vertical array data, but will not be reported further in this document.

4.2 The baseline model

A range independent seabed model of two homogeneous fluid seabed layers (*sediment* over *substrate*) was assumed. All parameters, fixed and those to be obtained by inversion, of the environment model are listed in Table 4.1.

Parameter		**Value**	**Unit**
Sound speed, water layer 1	Baseline	1484.0	m/s
Sound speed, water layer 2	Baseline	1471.0	m/s
Sound speed, water layer 3	Baseline	1461.0	m/s
Thermocline depth 1	Baseline	30.0	m
Thermocline depth 2	Baseline	275.0	m
Water depth	Inversion	RD	m
Density in water	Baseline	1.00	g/cm^3
P-wave velocity, sediment	Inversion	1770 (†)	m/s
Density, sediment	Inversion	2.00 (†)	g/cm^3
P-wave attenuation, sediment	Baseline	0.50	dB/λ
Thickness, sediment	Inversion	RD	m
P-wave velocity, substrate	Inversion	2400 (†)	m/s
Density, substrate	Baseline	2.20	g/cm^3
P-wave attenuation, substrate	Baseline	0.10	dB/λ

Table 4.1 Parameters of the environmental model. All parameters are labelled "baseline" or "inversion" to denote the manner in which they were obtained for subsequent work. RD denotes range dependent. A cross (†) denotes values of the baseline geophysical model (later replaced by values obtained by inversion of data).

A sound speed profile in water measured at the receiver position during the collection of the present acoustic data was stylised and sub-divided into three homogeneous layers. Parameters of these layers are listed in Table 4.1. The division into three layers and the thermocline depths were found relatively stable throughout the extent of the present part of the experiment. Baseline compressional (p-) wave velocities and densities of the two seabed layers are taken from the geoacoustic model of (20). Water depth and sediment thickness were dependent on

range. The p-wave attenuation parameters were selected in correspondence with values normally used for the Barents Sea.

4.3 Inversion parameters

The seven parameters included in the inversions were water depth, four seabed parameters and source range and depth (a small uncertainty in nominal positions). The inversion parameters, search intervals and number of values per parameter (equal size steps) are listed in Table 4.2.

Parameter	Unit	Range of values	Divisions	Step size
Water depth	m	(-15, +16.5)	64	0.5
Sediment thickness	m	6.5-38.0	64	0.5
Sediment p-speed	m/s	1500-1881	128	3
Sediment density	g/cm³	1.60-1.91	32	0.01
Substrate p-speed	m/s	1900-3790	64	30
Source range	m	(-90, +65)	32	5
Source depth	m	15.8-18.9	32	0.1

Table 4.2 Description, search intervals, number of subdivision per interval and step size for the parameters included in the inversions. Parenthesis indicates relative to a nominal value for each shot.

The reason for including small search intervals on the nominal source positions is to account for a possible small error on the nominal values reported from the experiment. Even though precise methods were used in the determination of these, a small residual error is expected.

Inversions were set up using four independent populations, each of sixty-four members. A total of 4096 forward models were tested per population. Other parameters of the genetic algorithm were set to nominal as recommended in the SAGA User's manual (16). Replica fields were generated using the range-independent OASES acoustic propagation model. The reason for using this model was its ability to handle seabed models of greater complexity (e.g. several seabed layers, elasticity in layers), which was a requirement for an inversion study conducted prior to the one reported here. Inversions took typically 2-3 hours on a 650 MHz twin-processor HP-7000 series computer. The *inversion model* is obtained as the maximum of the posterior probability distributions per parameter as computed by SAGA. In the version of the SAGA code used here (16), the models of the last generations of all populations of the genetic algorithm search are used in these computations. (A total of two hundred models were included in these estimations, that is, the fifty most fit members of each of four populations.)

4.4 Inversion results

The five geoacoustic model parameters estimated by inversion are listed in Table 4.3 for each of the shots used. The baseline values for the model parameters are listed in the bottom row. Table 4.3 also lists the Bartlett match associated with the estimated seabed models. This gives a measure of the correlation of measured and modelled acoustic data, that is, an indication of how well the replica field produced using the inversion model fits the actual data.

Shot Label	Nominal Range [km]	Water Depth [m]	Sediment Thickness [m]	Sediment p-velocity [m/s]	Sediment Density [g/cm³]	Substrate p-velocity [m/s]	Bartlett Match
E109 S	8.71	326.0	26.2	1569	1.80	2047	0.67
E115 S	3.20	322.0	26.4	1575	1.96	2078	0.45
W141 SM	-3.48	317.5	29.5	1581	1.79	2111	0.61
W127 S	-8.08	313.5	34.0	1632	1.70	3790*	0.69
W121 S	-13.19	285.0*	19.5	1605	1.74	3460	0.30
BASELINE				1770	2.00	2400	

Table 4.3 *Environment parameters estimated by matched-field inversion of shot data endfire to a 10-element horizontal array, using broadband incoherent Bartlett processor applied to five frequency components at 40 Hz-140 Hz. A star (*) indicates a value at a limit of the search interval. The nominal source range is indicated in the second column.*

It is observed that match is acceptably good for the four shots to a range of 8 km in either direction from the array. The match drops for the shot farther away at 13 km. Further results using shots at 16-20 km showed a similar drop in Bartlett match. Estimates of p-wave velocities in sediment and substrate obtained for the five shots are plotted in Figure 4.3.

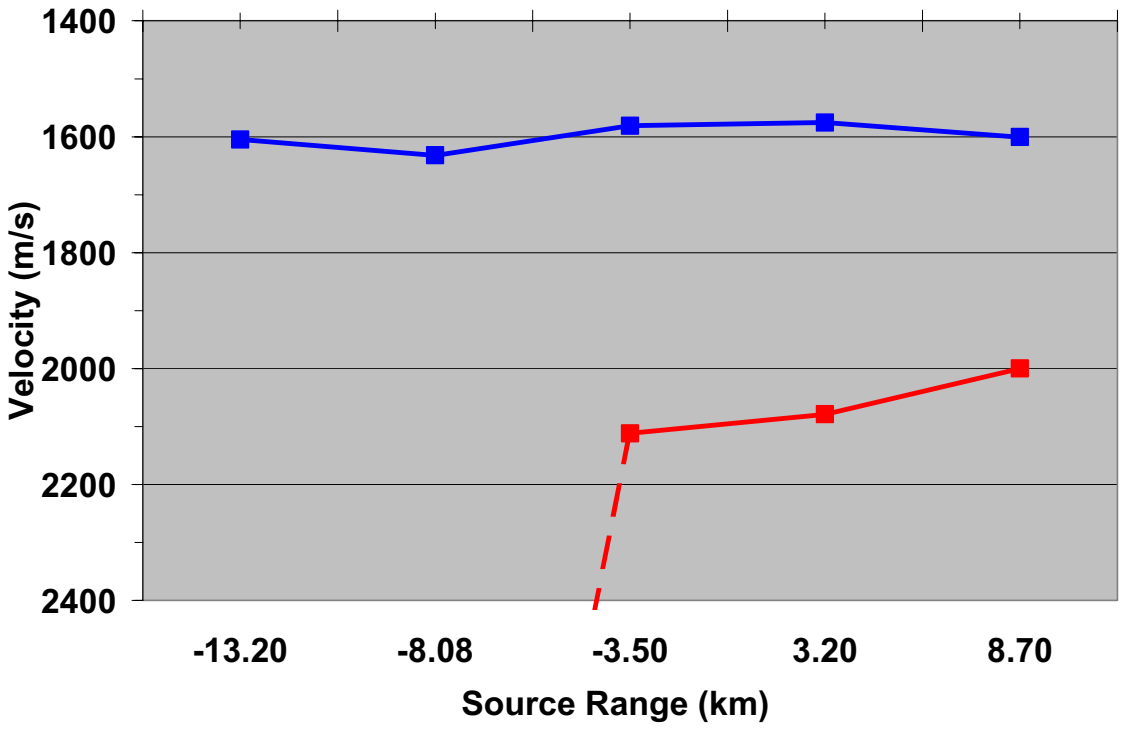

Figure 4.1 *Estimates of p-wave velocities in sediment (blue line and markers) and substrate (red line and markers) from matched-field inversion of multi-frequency shot data (40-140 Hz) endfire to 10-element bottom mounted horizontal array. Results are for five independent sources. Horizontal axis: range from nearest element of array, positive eastward.*

The p-wave velocity of sediment is consistently lower than baseline value, with a reduction in p-wave velocity from 1770 m/s to about 1600 m/s. The substrate p-wave velocity is less consistently estimated, with values of 2050-2100 m/s for three shots but higher values for the two farther shots in the westward direction. Estimates of density in sediment are consistently lower than the baseline value.

4.5 The optimal seabed model

Based on the results obtained, an optimal seabed model was constructed as shown in Table 4.4. This is based on an arithmetic average of results obtained from the first four shots of Table 4.3 (two shots at range 3 km and two shots at range 8 km in either direction from the array) for the p-wave velocity and density of sediment, an average value of sediment thickness for these ranges and an adjusted value for p-wave velocity in the substrate. The density in the substrate and the p-wave attenuations has been retained from the baseline model. The sediment thickness, although known to be range dependent both in the baseline model and from inversion of data, has been set to a fixed value.

Parameter	**Value**	**Baseline**	**Unit**
P-wave velocity in sediment	Inversion	1590	m/s
Density in sediment	Inversion	1.80	g/cm³
P-wave attenuation, sediment	Baseline	0.50 (†)	dB/λ
Thickness, sediment	Inversion	30.0	m
P-wave velocity in substrate	Inversion	2200	m/s
Density in substrate	Baseline	2.20 (†)	g/cm³
P-wave attenuation, substrate	Baseline	0.10 (†)	dB/λ

Table 4.4 Seabed model obtained by matched-field inversion of acoustic data to ranges 8 km from the horizontal array (four shots, two directions). A cross (†) denotes values retained from the baseline geophysical model.

The environment model used for source localization is composed the seabed model of Table 4.4, the sound speed profile in water of Table 4.2 and an optimised bathymetry.

5 SOURCE LOCALIZATION

5.1 Selection of data

The shots marked with an "L" in the last column of Table 3.1 were used for source localization. Thus a total of six shots at ranges 3-9 km in the two end-fire directions from the array and four shots at ranges 11-27 km in the westward direction were selected. Table 5.1 lists in the first three columns the shots; nominal source ranges and water depths measured at the nominal source ranges.

Frequency components were combined in two manners, which for the purpose are labelled *multi-frequency* and *broadband* processing. For both these applications, the incoherent broadband Bartlett processor is used. Individual single-frequency results were also computed but are not considered further. Localization using *multi-frequency* data made use of a small number of relatively widely spaced frequency components over the frequency span 40-140 Hz selected at peaks of the spectra (e.g. for shallow Mk-61 shots components were selected at 47.3, 65.8, 86.2, 105.9 and 120.2 Hz). Note that the selected frequency components are different from those used for inversion. Localization using *broadband* data employed using ten frequency components closely spaced within a 10 Hz wide band around a spectral peak in the interval 80-110 Hz alone or in combination with a 10 Hz wide band at a lower frequency.

Shot Label	Nominal range [km]	Water depth [m]
E109 S	8.73	342.8
E110 D	7.76	338.3
E115 S	3.20	325.5
Array Site	0.0	319.0
W139 SM	-3.21	310.7
W127 S	-7.24	303.0
W125 D	-9.00	296.3
W122 D	-11.51	297.3
W116 D	-16.53	286.5
W112 S	-19.83	284.3
W104 D	-26.44	277.3

Table 5.1 Shots used for localization, nominal source range and water depth measured at nominal source range. Range is positive eastward, measured from the closest element of the horizontal array.

5.2 Ambiguity surface computation

Ambiguity surfaces were computed using the C-SNAP forward model in range-independent mode, for a grid extending over 1.1-16.0 km in range and 1-300 m in depth (150 points in range at 100 m spacing and 100 points in depth at 3 m spacing, thus a total of 15.000 grid points), unless otherwise noted. The seabed model of Table 4.4 was used, with no variation of these parameters with range. Range dependence in bathymetry was approximated using an equivalent flat bathymetry representation (Eq. 2.9). Although source ranges in (2.9) are not known a priori, the grid ranges for which the value of the Bartlett processor is to be computed are known; thus the expression can be evaluated for each range step or a selection of steps of the ambiguity surface. The replica fields can then be computed using a range-independent forward model using an equivalent water depth at each such step. To further simply, the expression of Eq. 2.10 rather than Eq. 2.9 was used[2]. This procedure was adopted for all ambiguity surface computations, unless otherwise noted. By this procedure, the computations took less than 1 min on a 1.1 GHz Pentium III processor.

5.3 Multi-frequency processing

The incoherent broadband Bartlett processor was applied with data from five to eight frequency components over the interval 40-140 Hz. Six shots were processed. Results are shown in Table 5.2. The nominal ranges quoted in this and subsequent tables are to the closest element of the horizontal array. The numbers in parenthesis in the second column indicate the number of frequencies used in processing. The third column lists the value of the Bartlett processor, Equation (2.4), at the peak of the surface. Computation times were less than 60 seconds per surface on a 1.1 GHz processor.

Shot Label	Processing Frequencies [Hz]	Bartlett Match	Estimate Range [m]	Nominal Range [m]	Estimate Depth [m]	Nominal Depth [m]
E109 S	MF 40-120 (5)	0.55	8850	8727	12	18
E110 D	MF 47-137 (5)	0.62	7800	7764	78	86
E115 S	MF 40-120 (8)	0.37	3300	3205	18	18
W139 S	MF 40-140 (8)	-	-	3209	-	18
W127 S	MF 40-120 (8)	0.56	7300	7237	18	18
W125 D	MF 47-137 (8)	0.48	7600	8955	192	88

Table 5.2 Source range and depth estimation using matched-field processing of multi-frequency acoustic data (five to eight frequency components at 40-140 Hz), data recorded endfire to a 10-element bottom mounted horizontal array.

Results show that four of six shots were localized with a peak at correct range *and* depth: all three shots in the eastward direction and one of three shots in the westward direction. For shots E115 and W127 it was necessary to increase the number of frequencies included in the processing from five to eight; with five frequencies the sources were not localized. For shots

[2] Computations using the expression of (2.9) were not completed for this report.

W139 and W125 it was not possible to obtain correct estimates. Five of the ambiguity surfaces are plotted in Figure B.1.

5.4 Broadband processing

The incoherent broadband Bartlett processor was applied with data at ten frequency components over a 10 Hz band centred at a spectral peak within 80-110 Hz. Table 5.3 lists the position of the peak of the ambiguity surfaces. The centre frequency of the band used in processing is listed in the second column. Computation times were about 60 seconds per surface on a 1.1 GHz processor.

Shot Label	Processing Band [Hz]	Bartlett Match	Estimate Range [m]	Nominal Range [m]	Estimate Depth [m]	Nominal Depth [m]
E109 S	BB 108 (10)	0.52	8500	8727	96	18
E110 D	BB 090 (10)	0.49	7500	7764	12	86
E115 S	BB 105 (10)	0.28	3700	3205	39	18
W139 SM	BB 115 (10)	0.39	3100	3209	27	18
W127 S	BB 089 (10)	0.55	7600	7237	117	18
W125 D	BB 095 (10)	0.53	14300	8955	18	88

Table 5.3 Source range and depth estimation using broadband matched-field processing of acoustic data (ten frequency components from a 10Hz wide band centred at 80-110 Hz) recorded endfire to a 10-element bottom mounted horizontal array.

Results show that none of the shots were localized correctly. The error in range is in five of six cases to within a few cells of the nominal shot range, but with wrong depth estimates. For the two short-range shots E115 and W139, there is a peak close to the correct location, but at low Bartlett match. The corresponding ambiguity surfaces are plotted in Figure B.2. It is noted that there are many strong secondary peaks in each of the surfaces. Table 5.4 provides the location of the peak of each surface closest to the nominal source range. All listed peaks are to within 500 m in range of nominal, with three of these also correct in depth. The locations of further peaks of the ambiguity surfaces are tabulated in Appendix A.

Shot	Peak Order	Bartlett Match	Second peak [dB]	Estim. Range [m]	Nominal Range [m]	Range Error [m]	Estim. Depth [m]	Depth Error [m]
E109 S	2	0.48	-0.38	8800	8727	+100	18	0
E110 D	1	0.49	-	7500	7764	-300	12	-74
E115 S	1	0.28	-	3700	3205	+500	39	+21
W139 SM	1	0.39	-	3100	3209	-100	18	0
W127 S	2	0.52	-0.22	7200	7237	0	15	-3
W125 D	2	0.40	-1.43	9500	8955	+500	24	-64

Table 5.4 Same as Table 5.3, for peak of ambiguity surface closest to nominal source position in range. Fourth column is dB down from main peak of surface.

These results were obtained by use of data from a single 10 Hz wide band. Use of data from more 10 Hz bands will be treated next.

5.5 Multiple broadband processing

For the results obtained so far, data from a 10 Hz wide band centred at a spectral peak within 80-110 Hz was chosen. Figure 5.1 shows a set of spectra from all ten hydrophones of the horizontal array over the frequency interval 10 Hz–1 kHz (from shot W127). There are several additional peaks within the frequency interval of interest 40-140 Hz. A logical extension of the work so far is to include data from more bands in the processing.

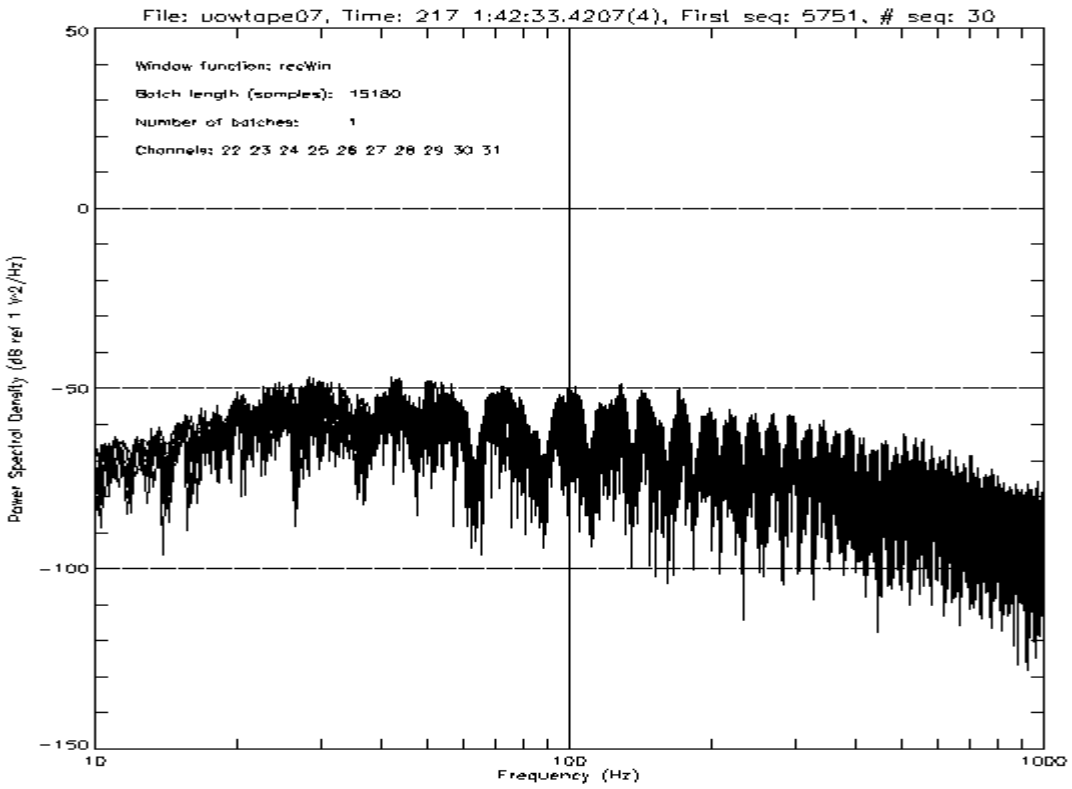

Figure 5.1 Typical frequency spectra from 10 hydrophones of the horizontal array. Frequency interval 10 Hz to1 kHz. From shot W127.

Data from a 10 Hz band within 80-110 Hz is combined with data from an adjacent band or with data from a 10 Hz band at a lower frequency. Eight shots from at ranges 3-27 km are treated. In order to reduce computational efforts, the equivalent water depth for the nominal source range *only* was used. The seabed model of Table 4.4, developed for the first eight km from the array, and a single sound speed profile in water as measured at the array site was used. Fully bathymetry-optimised ambiguity surfaces using the equivalent depth at *each* range step are subsequently computed in section 5.6.

5.5.1 Short-range shots

Two short-range shots detonated within 3 km of the array (E115 and W139) are treated. For these shots, results using one band of 10 Hz within 80-100 Hz were poor with low values of Bartlett match, even though range estimates close to the true were obtained. Here data from a second band at a lower frequency is added in processing. Results are shown in Table 5.5.

Shot Label	Processing Band [Hz]	Bartlett Energy [dB]	Estimate Range [m]	Nominal Range [m]	Estimate Depth [m]	Nominal Depth [m]
E115 S	BB 65+105 (15)	-4.76	3200	3205	15	18
W139 SM	BB 40+115 (21)	-4.19	3100	3209	18	18

Table 5.5 Source range and depth estimation using incoherent broadband Bartlett processor with acoustic data recorded endfire to a 10-element horizontal array at the seabed. The processing band(s) and total number of frequency components (in parenthesis) is listed in the second column.

Both shots are now located correctly in range *and* depth. There is a lower sidelobe level (secondary peaks –1.0 dB and –1.8 dB or more down from the main peak for the two shots respectively) than was achieved using data from a single band.

The low Bartlett energy for the main peak is attributed to two effects: the acoustic field at short range has a higher sensitivity to the seabed model and may require a more accurate forward model for replica field computations.

5.5.2 Medium-range shots

Table 5.6 lists results for shot W127 using two bands at 90 Hz and 110 Hz separately as well as from these two bands combined, and for shots W122 and W125, with data from bands at 40 Hz and 95 Hz used separately and combined. Similar computations were performed for shots E109 and E110 but results are not shown here.

Shot	Processing Band	Bartlett Energy	Estimate Range	Nominal Range	Estimate Depth	Nominal Depth
W127 S	BB 90 (10)	-2.57	7600	7237	117	18
W127 S	BB 110 (11)	-3.21	7600	7237	69	18
W127 S	BB 90+110 (21)	-3.27	7200	7237	21	18
W125 D	BB 40 (10)	-2.00	8900	8955	93	88
W125 D	BB 95 (10)	-2.67	14300	8955	21	88
W125 D	BB 40+95 (20)	-2.52	8900	8955	93	88
W122 D	BB 40 (8)	-1.26	15800	11514	99	86
W122 D	BB 95 (11)	-2.74	12300	11514	240	86
W122 D	BB 40+95 (19)	-2.53	11100	11514	72	86

Table 5.6 Same as Table 5.5. Shots W127, W125 and W122.

For shot W127, combining data from two bands, the peak of the ambiguity surface is at the correct location. For shot W125 using data at the 40 Hz band, the peak is at the correct location. This result is also obtained using the two bands combined, with the second peak -1.11 dB down from the main peak. For shot W122 the peak is at the correct location only when combining data from the two bands. The second peak is -0.62 dB down from the main peak. Selected ambiguity surfaces are plotted in Figure B.3.

5.5.3 Longer-range shots

For shot W116 at range 16.5 km and W112 at nominal range 19.8 km, additional low-frequency data at 16 Hz is included in the processing. The assumption is that the environment description of Table 4.4 becomes less accurate at longer range westward, but that low-frequency data will be less sensitive to this uncertainty. On the other hand, a lower resolution in depth and range is expected. Table 5.7 lists results for shot W116.

Shot	Processing Band	Bartlett Energy	Estimate Range	Nominal Range	Estimate Depth	Nominal Depth
W116 D	BB 16 (7)	-1.08	16700	16535	108	99
W116 D	BB 40 (10)	-1.84	16300	16535	264	99
W116 D	BB 80 (8)	-1.83	14800	16535	135	99
W116 D	BB 16+40 (17)	-2.04	16700	16535	105	99
W116 D	BB 40+80 (18)	-2.59	13300	16535	105	99
W116 D	BB 16+80 (15)	-2.56	16700	16535	135	99

Table 5.7 Same as Table 5.5. Shot W116.

Best results were obtained when using data from the 16 Hz and 40 Hz bands, the second peak of the ambiguity surface was -0.49 dB down from the main peak with a relatively small number of sidelobes. Processing including the 80 Hz band did not yield good results.

Table 5.8 lists the main peaks of the ambiguity surfaces for shot W112. Six of the ambiguity surfaces are plotted in Figure B.4.

Shot	Processing Band	Bartlett Energy	Estimate Range	Nominal Range	Estimate Depth	Nominal Depth
W112 S	BB 9 (8)	-0.91	19300	19832	6	18
W112 S	BB 16 (6)	-0.14	16300	19832	30	18
W112 S	BB 40 (8)	-1.19	20200	19832	21	18
W112 S	BB 80 (11)	-2.07	13700	19832	30	18
W112 S	BB 9+16 (14)	-1.74	20300	19832	51	18
W112 S	BB 9+80 (19)	-2.22	20300	19832	54	18
W112 S	BB 40+80 (19)	-1.87	20100	19832	24	18

Table 5.8 Same as Table 5.5. Shot W112.

The range estimate is overall improved from those obtained using a single broadband at 80 Hz; estimates are now all at 17-20 km in range. Best results were obtained when including data from the 40 Hz band in processing alone, the second peak of the surface is then -1.92 dB down from the main peak. For the ambiguity surface using the 40 Hz and 80 Hz bands, the second peak is -0.43 dB down. Also note that the main peaks are wider when using low-frequency data below 20 Hz; thus, a good depth resolution is not obtained using data from these bands alone. Finally, a shallow shot W104 at nominal range 27 km was selected. Data from three 10 Hz wide frequency bands centred at 20, 40 and 90 Hz was selected for processing. In addition, a low signal level band at 55 Hz (estimated 12-18 dB lower level) was included. Table 5.9 lists the main peaks of the ambiguity surfaces. Ambiguity surfaces are plotted in Figure B.5.

Shot	Processing Bands	Bartlett Energy	Estimate Range	Nominal Range	Estimate Depth	Nominal Depth
W104 D	BB 20 (7)	-3.29	26400	26440	153	83
W104 D	BB 40 (9)	-1.18	27100	26440	90	83
W104 D	BB 55 (10)	-4.87	27000	26440	36	83
W104 D	BB 90 (9)	-2.45	31300	26440	156	83
W104 D	BB 20+40 (16)	-2.08	27100	26440	90	83
W104 D	BB 20+90 (16)	-3.23	29700	26440	51	83
W104 D	BB 40+55 (19)	-2.87	27100	26440	84	83
W104 D	BB 55+90 (19)	-4.43	29100	26440	222	83
W104 D	BB 20+40+90	-2.87	27100	26440	90	83

Table 5.9 Same as Table 5.6. Shot W104.

Best results were obtained when including data from the 20 Hz and 40 Hz bands, the second peak of the ambiguity surface is then -0.96 dB down from the main peak. The peak is at correct depth but offset 700 m in range. Including also data from the 90 Hz band, the second peak was -0.79 dB down. Processing using the low-level 55 Hz band alone yielded a good range estimate with a very broad main lobe almost 2.0 dB above the secondary peak, but at a low value of Bartlett energy.

5.6 Summary of results

Table 5.10 and Figure 6.1 summarises results obtained for all ten shots using broadband processing of acoustic data at 40 Hz-140 Hz. The frequency content of the data used is listed in the second column of the table, with the number in parenthesis indicating the total number of frequency components included.

Shot Label	Processing Band [Hz]	Bartlett Match	Second Peak [dB]	Estimate Range [m]	Nominal Range [m]	Estimate Depth [m]	Nominal Depth [m]
E109 S	BB 40+108 (20)	0.49	-1.71	8800	8727	18	18
E110 D	BB 40+90 (21)	0.55	-1.11	7900	7764	84	86
E115 S	BB 65+106 (15)	0.33	-1.00	3200	3205	15	18
W139 S	BB 40+114 (21)	0.39	-1.80	3100	3209	18	18
W127 S	BB 40+90 (21)	0.47	-0.81	7200	7237	24	18
W125 D	BB 40+95 (20)	0.56	-1.02	8900	8955	93	88
W122 D	BB 40+65 (19)	0.63	-0.47	11600	11514	87	86
W116 D	BB 40+60 (17)	0.63	-0.20	16600	16535	105	99
W112 S	BB 40+80 (20)	0.65	-1.18	20100	19832	24	18
W104 D	BB 40+55 (16)	0.51	-1.20	27100	26440	84	83

Table 5.10 Summary of matched-field localization results obtained using incoherent broadband Bartlett processor applied to shot data recorded endfire to a 10-element bottom mounted horizontal array from the 1999 experiment in the Barents Sea. Ten shots at ranges 3-27 km, data from two10 Hz wide bands within 40-110 Hz. Processing bands centre frequencies listed in second column.

All these results were obtained using the seabed model obtained by matched-field inversion of acoustic data, and for bathymetry-optimised ambiguity surfaces using the geometric mean water depth for *each* range step. Computation of these surfaces took less than 60 sec on a 1.1 GHz processor in all cases. The error in estimated range is plotted in Figure 5.2. Ambiguity surfaces for four selected shots are plotted in Figure 5.3.

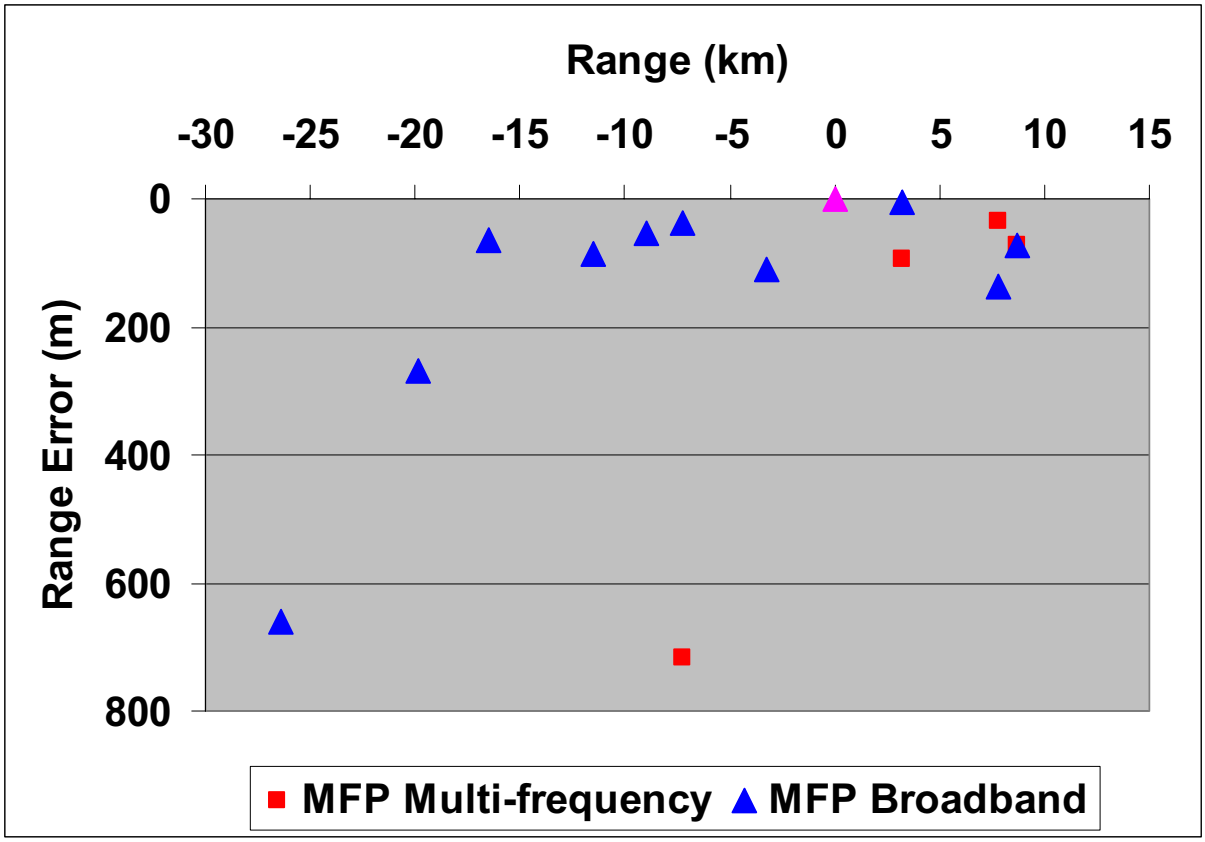

Figure 5.2 *Error in MFP range estimate obtained using incoherent broadband Bartlett processor applied to shot data recorded end-fire to a 10-element bottom mounted horizontal array from the 1999 experiment in the Barents Sea. Results obtained for ten shots at ranges 3-27 km from the array, using multi-frequency processing (five frequency components at 40-140 Hz, red squares) and broadband processing (two 10 Hz wide bands centred at 40Hz - 110 Hz, blue triangles). Depth estimates are for all shots within 6 m of nominal. The array site is marked by a pink triangle.*

All eight shots at ranges 3-17 km have been localized to within 200 m in range *and* to within 6 m in depth using broadband processing. Two long-range shots at 20 km and 27 km have been localized to within 700 m in range and 6 m in depth.

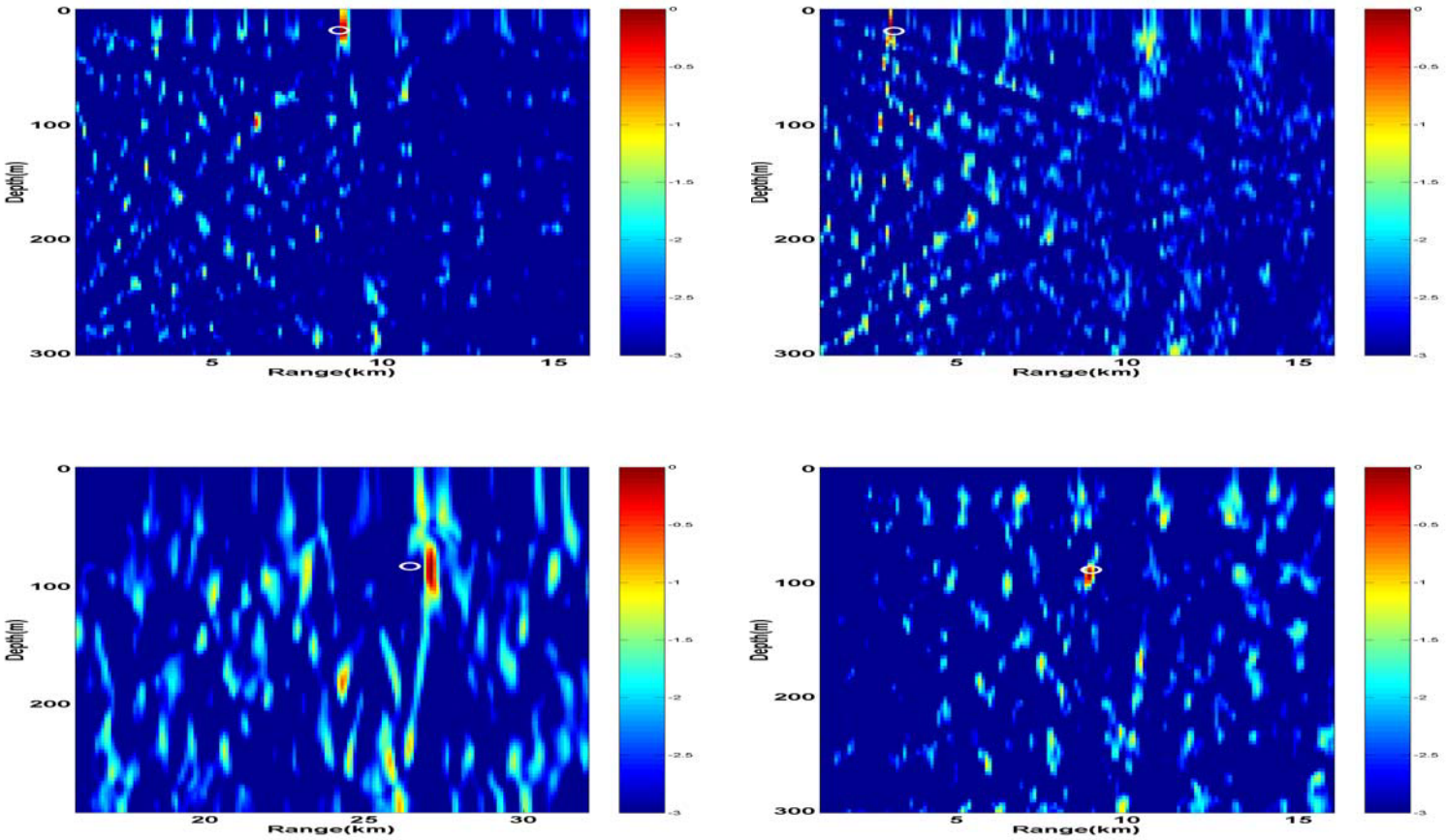

Figure 5.3 *Range-depth ambiguity surfaces using incoherent broadband Bartlett processor applied to shot data recorded endfire to a 10-element bottom mounted horizontal array. Shots at range 8 km east (upper left), 3 km west (upper right), 9 km west (lower right) and 27 km west (lower right). Dynamic range is 3 dB. White circles indicate nominal source positions.*

6 SUMMARY AND DISCUSSION

Matched-field processing techniques have been applied to explosive source data recorded endfire to a bottom mounted horizontal array. A two-step approach to source localization was employed. The first step, focusing the environment, was performed using matched-field inversion for seabed parameters using the incoherent broadband Bartlett processor with multi-frequency data at frequencies from 40 Hz to 140 Hz from known sources. The second step, localization, was performed using the ambiguity surface method, with replica fields computed using a range-independent normal mode propagation model (C-SNAP) for an optimised model environment. A range-independent seabed model and an optimal water depth computed for a constant-slope bathymetry was used.

Ten shots at nominal ranges from 3 km to 27 km in two directions end-fire to the array were examined. The incoherent broadband Bartlett processor was used with frequency content in two manners: with five to eight frequency components over the interval 40-140 Hz and with data from two 10 Hz wide bands (ten frequency components from each band) centred within 40-110 Hz. Eight shots at short to medium ranges (3 to 17 km) were localized to within 200 m in range using broadband processing. Two shots at longer ranges (at 20 km and 27 km) were localized to within 700 m in range. The shots were also correctly localized in depth when data from two 10 Hz bands was combined. Better than expected, all shots were localized to within 6 m in depth. Both shallow (nominal depth 18 m) and deep (nominal depth 91 m) sources were treated. A typical Bartlett match of 0.50 to 0.65 was achieved, with a typical peak-to-sidelobe separation of –1.0 dB or better, deteriorating slightly with range[3].

The general understanding that use of incoherent broadband averaging provides more stable results has been demonstrated in the present work. The observation is also made that broadband processing using 10 Hz wide bands stabilised the results over those obtained using processing with fewer and more widely spaced frequency components. The frequency bands centred at 40 Hz and at 80-110 Hz were chosen rather arbitrarily and may not have been the best choices. The selection of processing frequencies and requirements to HLA array design (both array length and element spacing) has not been further addressed in the present work.

One practical issue when using a range-independent forward model for a range-dependent bathymetry environment is the determination of an effective model water depth. It was found that using the geometric mean between the water depth at the array position and at a number of pre-determined ranges or each grid step in range provided good results. This is achievable in practice where the bathymetry of the area has been measured; also the slope of bathymetry must be small. It is suggested that the next step in analysis of the present data should include use of a fully range-dependent forward model. This should eliminate the issue of selecting a model water depth, but at the cost of higher processing time.

[3] The sidelobe levels in MFP should not be directly compared with levels in classical array design.

Care was taken in determining a seabed model for the area of experiment. Yet, an underlying problem of mismatch may prevail and warrant further research. Possible contributors to mismatch that have not been addressed in the present work are: imperfect knowledge of array element positions, variation of sound speed profile in water with range dependence and further mismatch in the seabed model. The problem of mismatch seemed to be of more concern at longer range, where the variability may be greater than that incorporated in the environment model as developed for the present work.

It would be of interest to include one or a few elements of the VLA combined with data from the HLA in the processing to determine if a better resolution in depth can be obtained with use of less data or with data from a shorter segment of the HLA. This report treated shots recorded endfire to the horizontal array, thus at an a priori known direction. Extension of the methods presented to sources in directions off endfire should also be further investigated.

References

(1) H P Bucker (1976): Use of calculated sound fields and matched-field detection to locate sound in shallow water, *J. Acoust. Soc. Am.* **59**, 368-373.

(2) R G Fizell (1987): Application of high-resolution processing to range and depth estimation using ambiguity function methods, *J Acoust Soc Am* **82**, 606-13.

(3) A B Baggeroer, W A Kuperman and H Schmidt (1988): Matched field processing: Source localization in correlated noise as an optimum parameter estimation problem, *J Acoust Soc Am* **83**, 571-587.

(4) J M Ozard (1989): Matched field processing in shallow water for range, depth, and bearing determination: Results of experiment and simulation, *J Acoust Soc Am* **86**, 744-53.

(5) M D Collins and W A Kuperman (1991): Focalization: environmental focusing and source localization, *J Acoust Soc Am* **90**, 1410-1422.

(6) N R Chapman and M L McKirdy (1992): Matched field source localization using broadband shot data, Defence Research Establishment Pacific, unpublished manuscript.

(7) S M Jesus (1993): Broadband matched-field processing of transient signals in shallow water, *J Acoust Soc Am* **93**, 1841-1850.

(8) R K Brienzo and W S Hodgkiss (1993): Broadband matched-field processing, *J Acoust Soc Am* **94**, 2821-2831.

(9) P Gerstoft (1994): Inversion of seismoacoustic data using genetic algorithms and a posteriori distributions, *J Acoust Soc Am* **95**, 770-782.

(10) P Gersoft and D F Gingras (1996): Parameter estimation using multifrequency range-dependent acoustic data in shallow water, *J Acoust Soc Am* **99**, 2839-2850.

(11) N O Booth, P A Baxley, J A Rice, P W Schey, W S Hodgkiss, G L D'Spain, J M Murray (1996): Source localization with broad-band matched-field processing in shallow water, *IEEE J Oceanic Engineering* **21**, 4, 402-412.

(12) P Zakarauskas, S E Dosso and J A Fawcett (1996): Matched-field inversion for source location and optimal equivalent bathymetry, *J Acoust Soc Am* **100**, 1493-1500.

(13) R Chapman and M Taroudakis (eds.) (2000): Geoacoustic inversion in shallow water, *J Computat Acoustics* **8**, 2.

(14) A Tolstoy (1993): Matched field processing for underwater acoustics, World Scientific, Singapore.

(15) F B Jensen, W A Kuperman, M B Porter, H Schmidt (2000): Computational ocean acoustics, Springer Verlag, New York.

(16) P Gerstoft (1999): SAGA User Manual 3.0: An inversion software package, SACLANT Undersea Research Centre and Marine Physical Laboratory.

(17) C M Ferla, M B Porter and F B Jensen (1993): C-SNAP: Coupled SACLANTCEN normal mode propagation loss model, SACLANTCEN memorandum SM-274.

(18) E J Eidem, B Bendiksen, H Helgesen (1999): Project SWASI: Technical cruise report from phase S-V 1999, FFI/RAPPORT-99/04955

(19) E J Eidem (2000): Estimation of the hydrophone array position during SWASI 1999 phase S-V, FFI/RAPPORT-2000/04107

(20) C E Solberg (2001): Geoakustiske modeller for MFP eksperimentet i Barentshavet 1999 (in norwegian), FFI/RAPPORT-2001/00335

(21) E J Eidem (2001): Single shot inversion from the L-antenna experiment in 1999, FFI/RAPPORT-2001/02927

(22) E J Eidem (2002): Broadband inversion and source localization of vertical array data from the L-antenna experiment in 1999, FFI/RAPPORT-2002/02565

APPENDIX

A AMBIGUITY SURFACE TABLES

A.1 Secondary peaks

The ambiguity surfaces computed in section 5.4 are treated. The location the main and two secondary peaks of the ambiguity surfaces as well as the dB value (Bartlett Energy) of these is listed in Tables A.1-A.2 for four shots. For broad peaks extending typically over one or two adjacent cells in range and two or three adjacent cells in depth, only the values at the centre of such are listed. The position closest to the true source in range is marked with an asterisk.

Shot Label	Peak number	Bartlett Energy [dB]	Range [m]	Depth [m]
E109 S	1	-2.80	8500	96
	2*	-3.18	8800	18
	3	-3.65	8200	6
W127 S	1	-2.57	7600	117
	2*	-2.79	7200	15
	3	-2.80	7200	198

Table A.1 Peaks of ambiguity surface using broadband processing (10 Hz band at about 100 Hz). Shallow sources.

Shot Label	Peak number	Bartlett Energy [dB]	Range [m]	Depth [m]
E110 D	1*	-3.05	7500	12
	2	-4.15	5500	12
	3	-4.69	10200	25
W125 D	1	-2.69	14300	18
	2*	-4.12	9500	24
	3	-4.18	7000	15

Table A.2 Peaks of ambiguity surface using broadband processing (10 Hz band at about 100 Hz). Deep sources.

A.2 Ambiguity surfaces in segments

In an effort to reduce computation time, replica fields can be computed in segments for a few a priori selected ranges. The procedure is applied to broadband data. The model water depth for the replica field computations is set to the geometric mean computed for three ranges at 4.0 km, 8.0 km and 16.0 km. The procedure entails computing ambiguity surfaces for these segments separately, then selecting the peak of highest Bartlett value among these surfaces. This procedure may also be applied in areas where the bathymetry is known only at a few points in range.

This multi-step procedure is demonstrated using three segments:

- ranges 1.1-8.0 km using geometric mean water depth at 4.0 km
- ranges 6.1-10.0 km using geometric mean water depth at 8.0 km
- ranges 10.1-16.0 km using geometric mean water depth at 12.0 km.

The peaks of the ambiguity surfaces for either of these computations are listed in Tables A.4-A.6. Results are combined by selecting the peak within the three ambiguity surfaces of highest Bartlett energy. Results for five shots are summarised in Table A.3-A.6. Computation times using this method was less than 2 sec on a 1.1 GHz processor, thus at a computation time reduced by a factor of 40 compared with fully bathymetry-optimised surfaces. Results are comparable to those obtained in Table 5.3. The procedure will rely on a pre-selection of a few ranges for which to compute surfaces.

Shot Label	Processing Band [Hz]	Bartlett Energy [dB]	Estimate Range [m]	Nominal Range [m]	Estimate Depth [m]	Nominal Depth [m]
E109 S	BB 108	-2.73	9650	8727	9	18
E110 D	BB 090	-3.00	7300	7764	12	86
E115 S	BB 106	-4.76	3100	3205	3	18
W127 S	BB 108	-2.61	7100	7237	30	18
W125 D	BB 095	-2.59	11000	8955	225	88

Table A.3 Best of three ambiguity surfaces computed for three segments with geometric mean water depth to 4.0, 8.0 and 12.0 km. Broadband data from a 10 Hz wide frequency band centred at 80-110 Hz.

Shot	Processing Band [Hz]	Bartlett Energy	AS-max Range	Nominal Range	AS-max Depth	Nominal Depth
E109 S	BB 108	-3.16	7750	8727	192	18
E110 D *	BB 090	-3.00	7300	7764	12	86
E115 S *	BB 106	-4.76	3100	3205	3	18
W127 S	BB 108	-2.82	7900	7237	123	18
W125 D	BB 095	-3.21	6900	8955	63	88

Table A.4 Location of peak of ambiguity surface computed for range segment 1.1-8.0 km, water depth set to geometric mean for 4.0 km.

Shot	Processing Band [Hz]	Bartlett Energy	AS-max Range	Nominal Range	AS-max Depth	Nominal Depth
E109 S	BB 108	-2.77	8450	8727	96	18
E110 D	BB 090	-3.23	7550	7764	12	86
E115 S	BB 106	-5.97	7950	3205	84	18
W127 S *	BB 108	-2.61	7100	7237	30	18
W125 D	BB 095	-3.01	9000	8955	129	88

Table A.5 *Same as Table A.4, range segment 6.1-10.0 km, water depth set to geometric mean for 8.0 km.*

Shot	Processing Band [Hz]	Bartlett Energy	AS-max Range	Nominal Range	AS-max Depth	Nominal Depth
E109 S *	BB 108	-2.73	9650	8727	9	18
E110 D	BB 090	-3.63	8150	7764	12	86
E115 S	BB 106	-6.32	8450	3205	90	18
W127 S	BB 108	-2.79	10850	7237	12	18
W125 D *	BB 095	-2.59	11000	8955	225	88

Table A.6 *Same as Table A.4, range segment 8.1-16.0 km, water depth set to geometric mean for 12.0 km.*

B AMBIGUITY SURFACE PLOTS

Ambiguity surfaces are plotted using the Bartlett energy in dB. In all plots, the dB scale is set relative to the maximum (the *peak*) of the ambiguity surface. A dynamic scale of -3 dB down from the peak is used in all plots. The nominal position of the source is indicated with a white circle in some but not all of the plots. The nominal positions are also listed in Table B.1.

Shot Label	Nominal Range [m]	Nominal Depth [m]
E109 S	8727	18
E110 D	7764	86
E115 S	3205	18
W139 S	3209	18
W127 S	7237	18
W125 D	8955	88
W122 D	11514	86
W116 D	16535	99
W112 S	19832	18
W104 D	26440	83

Table B.1 Source nominal range and depth.

B.1 Multi-frequency processing

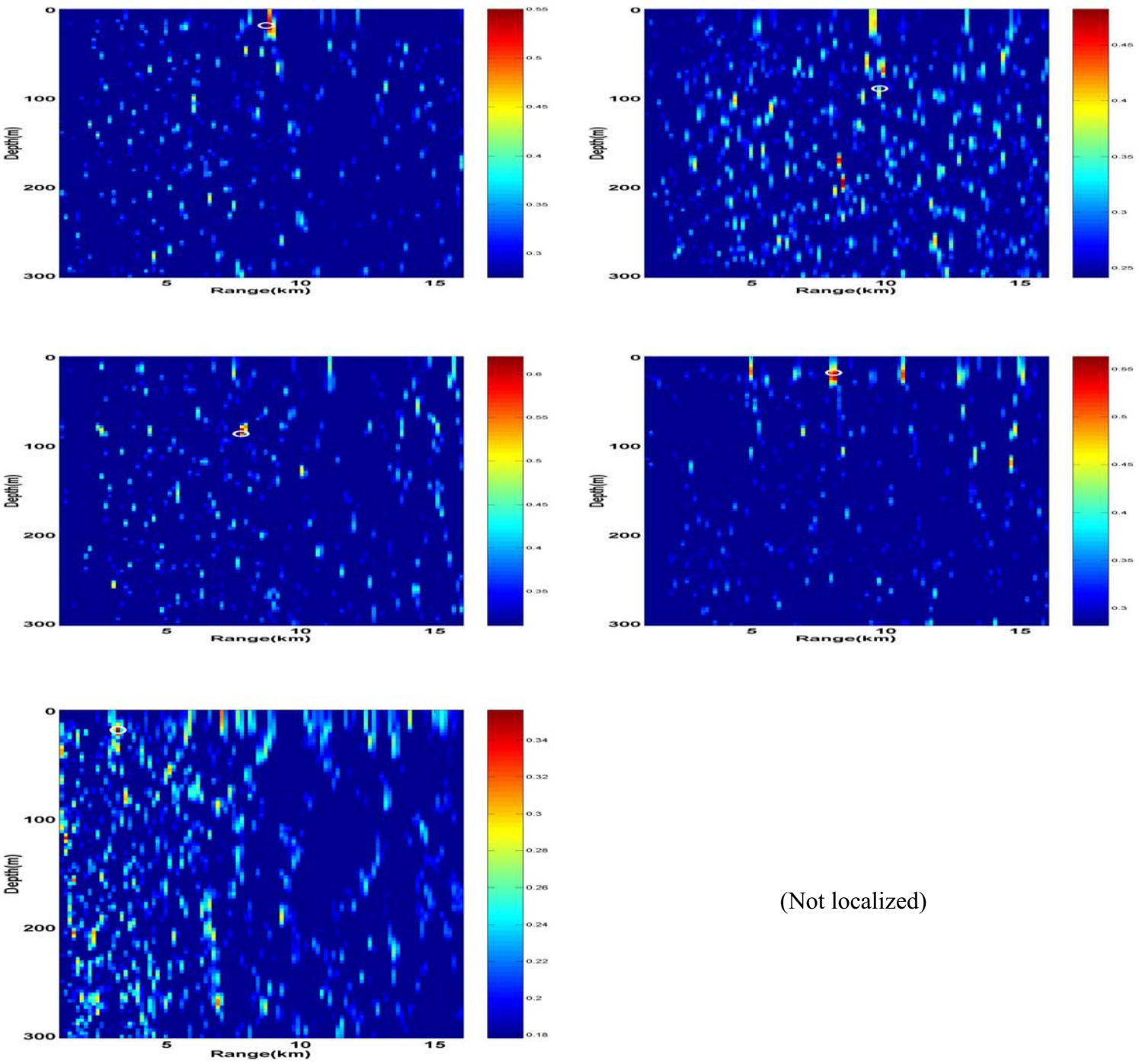

Figure B.1 *Range-depth ambiguity surfaces using multi-frequency incoherent Bartlett processor (40-140 Hz) applied to shot data recorded end-fire to a 10-element bottom mounted horizontal array. Shots at ranges 8 km (upper panels), 7 km (middle panels) and 3 km (lower panels) from eastward (left panels) and westward (right panels) tracks.*

B.2 Broadband processing

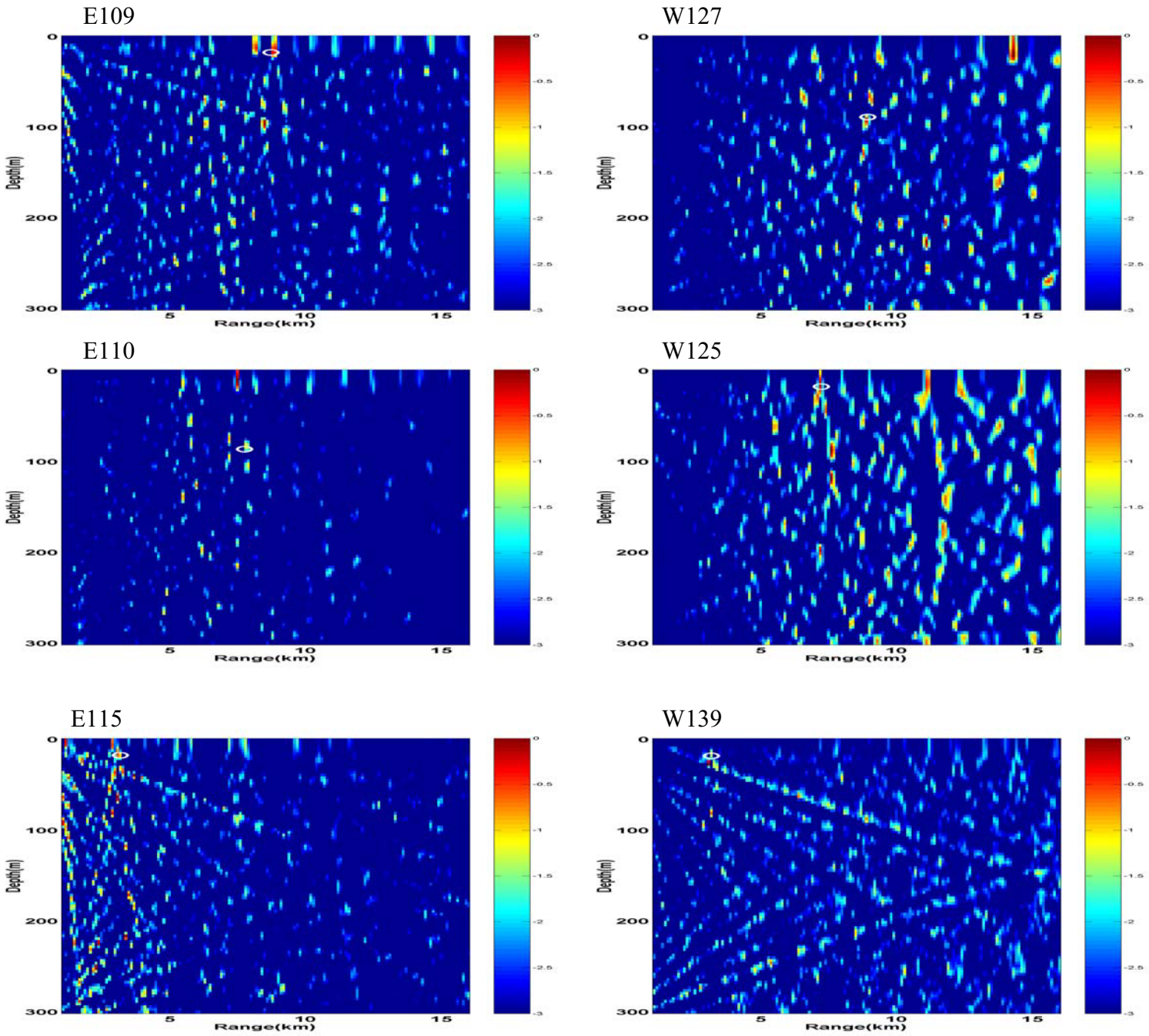

Figure B.2 Range-depth ambiguity surfaces using broadband incoherent Bartlett processor (10 Hz band centred at 80-110 Hz) applied to shot data recorded end-fire to a 10-element bottom mounted horizontal array. Shots at ranges 8.9 km (upper panels), 7.2 km (middle panels) and 3 km (lower panels) from eastward (left panels) and westward (right panels) tracks.

B.3 Multiple broadband processing

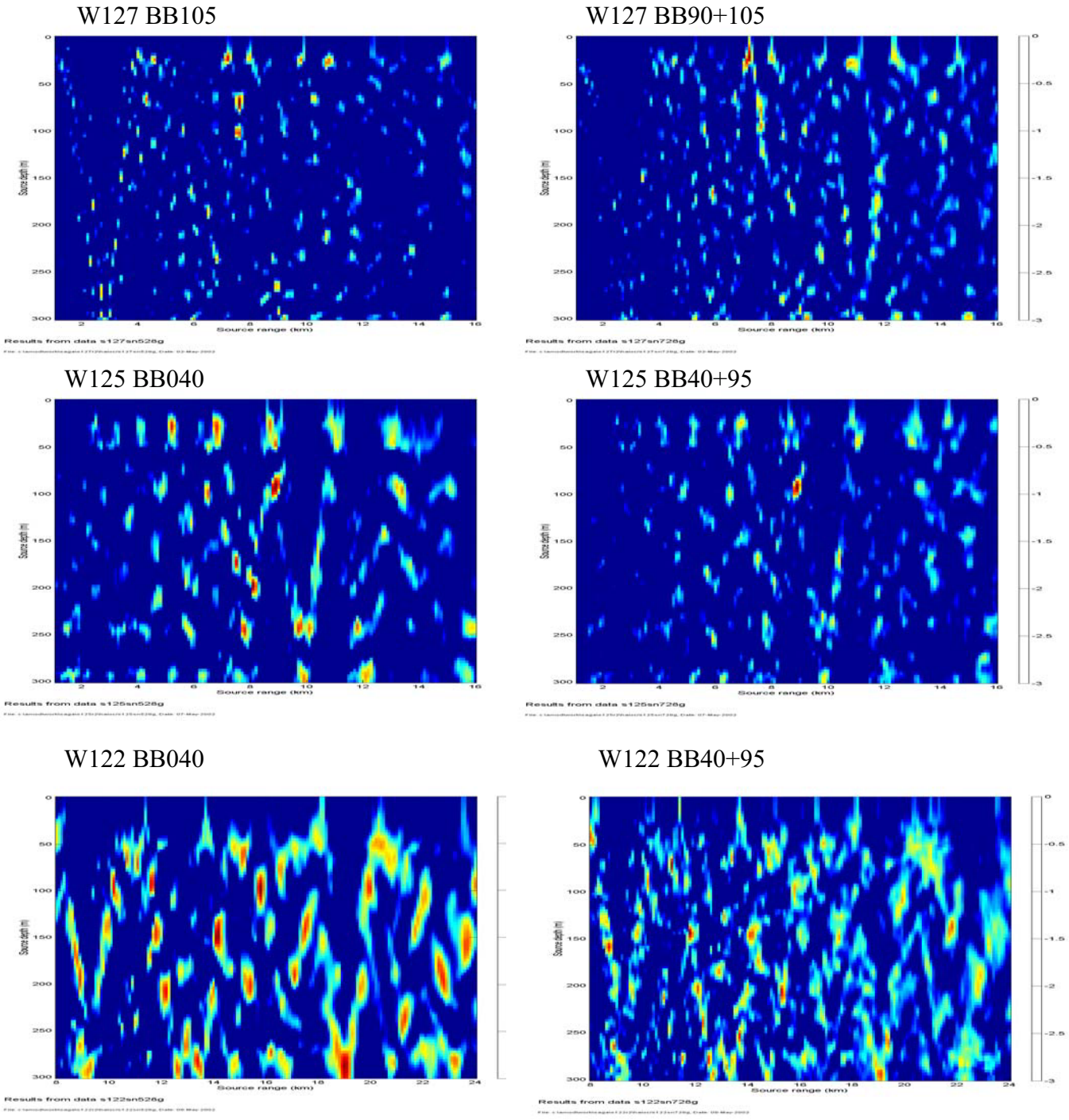

Figure B.3 Range-depth ambiguity surfaces using a single 10 Hz frequency band (left panels) and combination of two bands (right panels). Shot data at ranges 7.2 km (upper panels), 8.9 km (middle panels) and 11.5 km (lower panels) recorded end-fire to 10-element bottom mounted horizontal array.

B.4 Multiple broadband processing (shot W112)

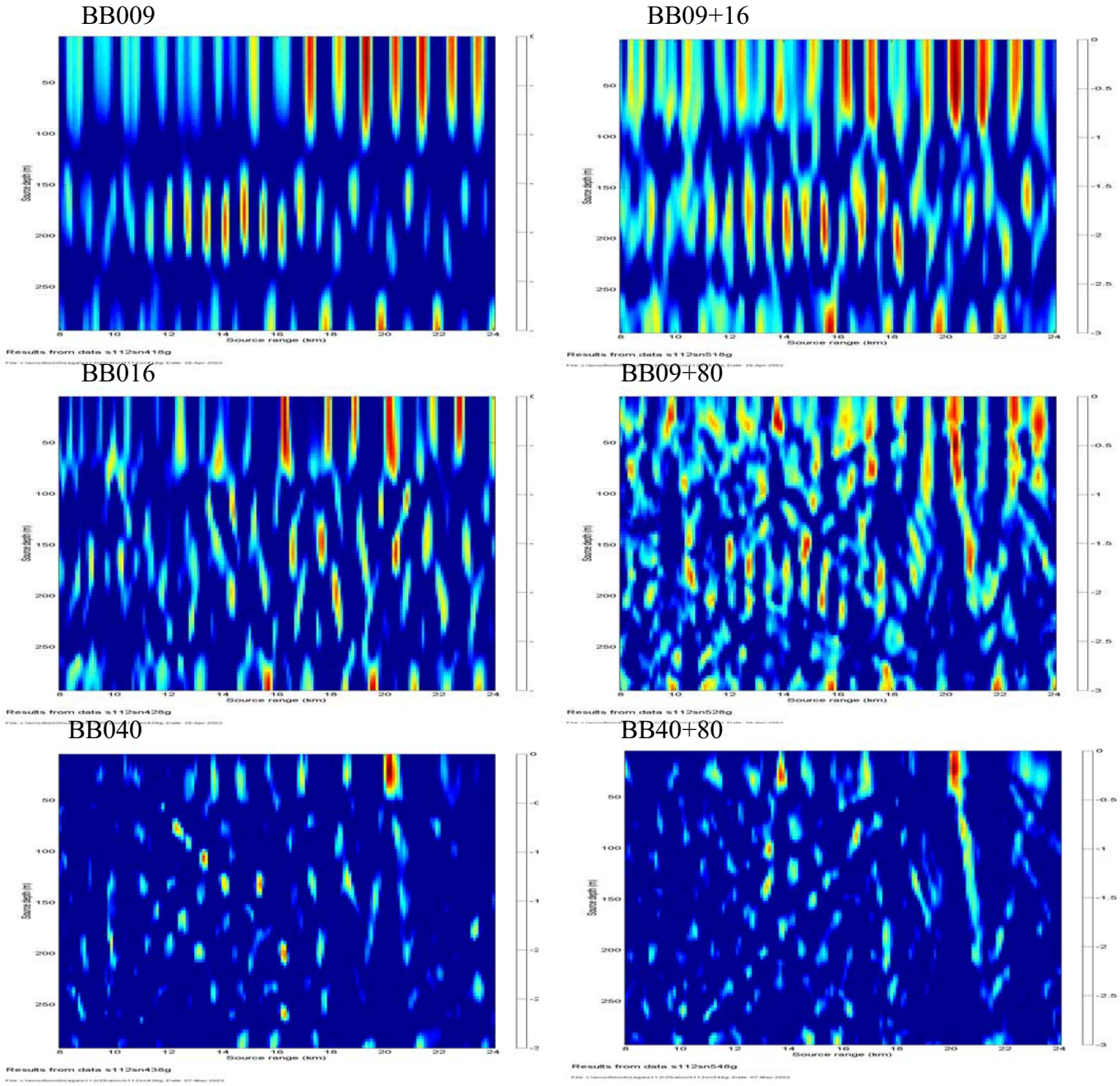

Figure B.4 Range-depth ambiguity surfaces using broadband shot data recorded at range 19.8 km end-fire to 10-element bottom mounted horizontal array. Broadband processing using bands centred at 9 Hz (upper left), 16 Hz (middle left) and 40 Hz (lower left), and a combination of two bands at 9+16 Hz (upper right), 9+80 Hz (middle right) and 40+80 Hz (lower right).

B.5 Multiple broadband processing (shot W104)

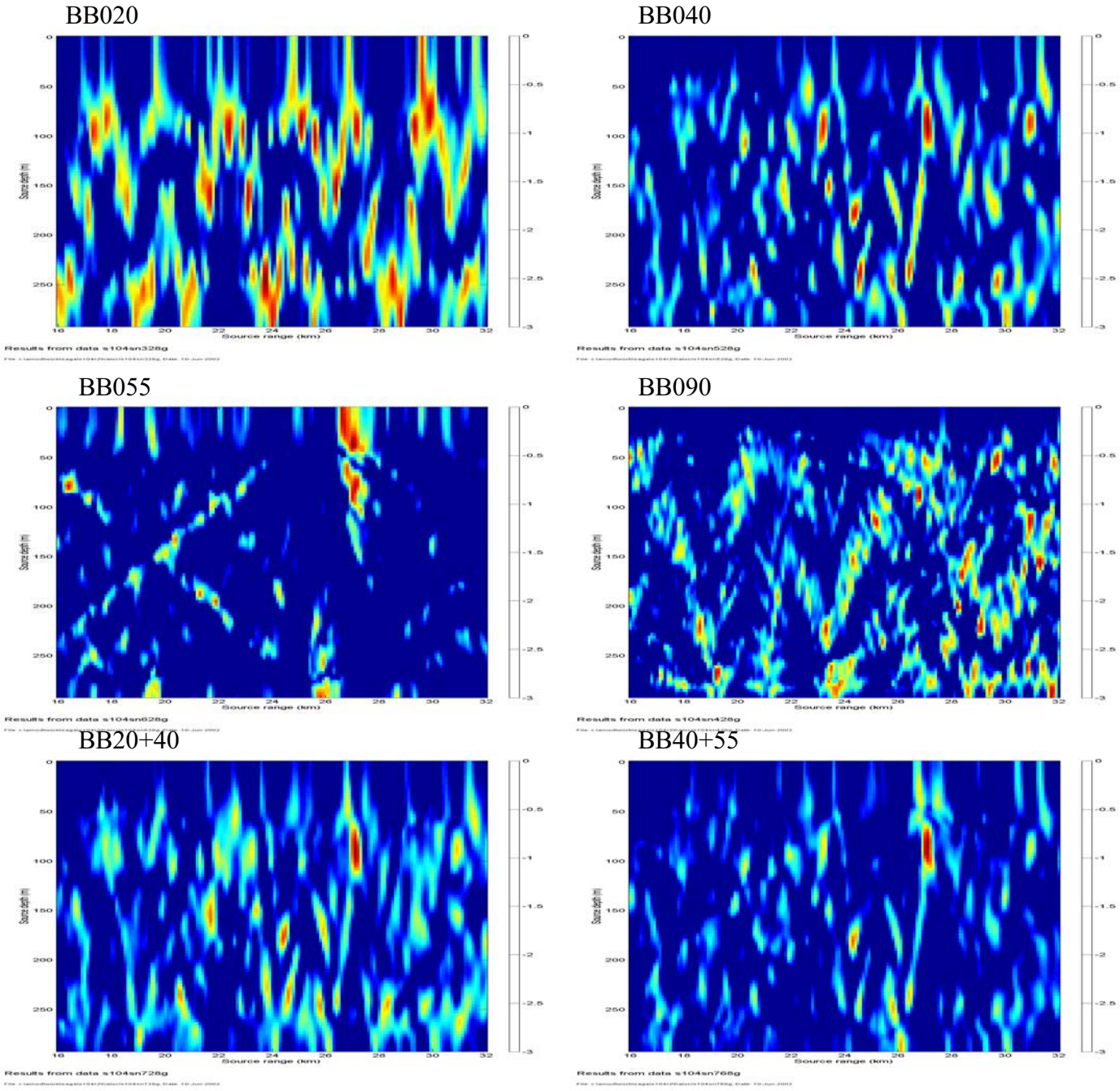

Figure B.5 *Range-depth ambiguity surfaces using broadband shot data recorded at range 26.4 km end-fire to 10-element bottom mounted horizontal array. Broadband processing using bands centred at 20 Hz (upper left), 40 Hz (upper right) and 55 Hz (middle left) and 90 Hz (middle right), and a combination of two bands at 20+40 Hz (lower left) and 40+55Hz (lower right).*

C FOCALIZATION

The procedure of localizing a source and optimising environmental parameters in a combined process, *focalization*, was introduced by Collins and Kuperman (5) and has subsequently been applied by several researchers. Here the method is applied to source localization when also optimising for effective water depth (section C.1) and thermocline depth (section C.2).

C.1 Focalization including bathymetry

A global search method (genetic algorithm of SAGA) is employed, with the water depth, source range and source depth as the three search parameters. A small search interval on water depth of +/-6.0 m around the geometric mean depth to a range of 8.0 km was used. A total of 2000 models were tested (search interval in range 4-12 km; range increment 50 m, water depth increment 0.2 m). The range-independent version of the C-SNAP propagation model was used. The seabed model was as fixed by matched-field inversion of acoustic data. Shot data from a 10 Hz wide band centred at 90-110 Hz was used for four shots at ranges 7-8 km from the array. The computation time for this application increases since the replica fields have to be re-computed for every new trial value of water depth.

The estimates of water depth, source range and source depth for the best-of-all model of the search are quoted in Table C.1. The optimisations took about 15 min each on a 1.1 GHz processor. The two shallow shots (E109 and W127) were localized.

Shot	Processing Band [Hz]	Bartlett Energy [dB]	Water Depth Estimate	Range Estimate [m]	Nominal Range [m]	Depth Estimate [m]	Nominal Depth [m]
E109 S	BB 110	-2.84	330.5	8850	8727	15	18
E110 D	BB 90	-3.66	323.9	5600	7764	51	86
W127 S	BB 110	-2.36	315.7	7300	7237	30	18
W125 D	BB 95	-3.19	307.1	7150	8955	39	88

Table C.1 Source range and depth and water depth estimated by global search. Data from a 10 Hz wide band at 80-110 Hz.

C.2 Focalization including bathymetry and thermocline depth

The thermocline depth and water depth is included in the optimisation. This parameter was kept fixed at nominal value in the previous work. The total number of parameters in the global search is thus four: water depth, thermocline depth, source range and source depth. The search interval of the thermocline depth was set to 22.0-34.0 m, which is +/-6.0 m of the nominal value. The thermocline depth was not linked to the water depth. For this larger search space, the number of tested models was now increased to 8000. The computations took about 1 hour. Seven shots were treated. Results are listed in Table C.2.

Shot	Processing Band [Hz]	Bartlett Energy [dB]	Water Depth Estim.	Therm ocline Estim.	Range Estim. [m]	Nominal Range [m]	Depth Estim. [m]	Nominal Depth [m]
E109 S	BB 110	-2.57	325.9	29.5	8600	8727	12	18
E110 D	BB 90	-2.92	327.1	30.4	7450	7764	12	86
W127 S	BB 110	-2.70	307.3	31.3	7050	7237	15	18
W125 D	BB 95	-3.68	316.1	22.3	7600	8955	42	88
W122 D	BB 95	-2.59	310.3	30.7	12500	11514	237	86
W126 D	BB 40+80	-1.92	306.5	22.6	17100	16535	105	99
W112 S	BB 80	-1.78	304.2	22.0	20600	19832	15	18

Table C.2 Same as Table C.1, optimising also for thermocline depth. Data from a 10 Hz wide band at 80-110 Hz.

The quoted values are now the maximum of the posterior probability distributions as estimated by SAGA. The marginal posterior probability distributions for each of the four optimised parameters as estimated by SAGA are plotted in Figure C.1. Three shallow and one deep shot was localized in range and depth. Range estimates are to within 300 m for shots to a range of 9 km and to within 1000 m for longer-range shots. Compared with the results optimising only for source position and water depth, an improved localization in depth has been achieved.

Search Parameters	Number of models	Computer time [min]
Source range Source depth Water depth	2000	11
Source range Source depth Water Depth Thermocline depth	8000	60

Table C.3 Execution times for focalization runs.

Results would be expected to improve by addition of more data in the processing. The method could be extended to include all environment parameters including the seabed parameters, but this would require testing more models and thus a further increase in computation time.

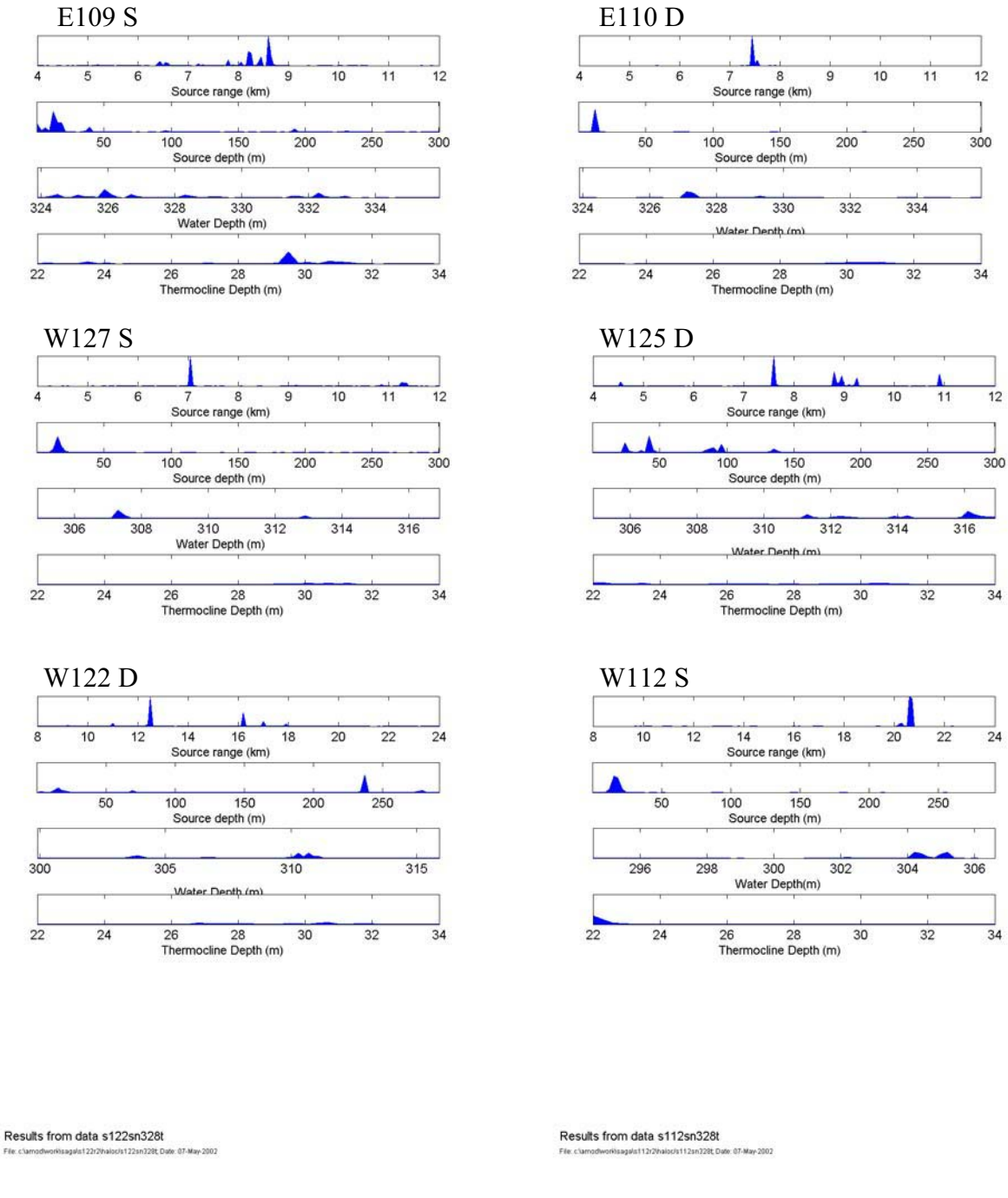

Figure C.1 Posterior probability distributions for parameters included in optimisation for source range and depth, water depth and thermocline depth. Shots are E109 (upper left), E110 (upper right), W127 (middle left), W125 (middle right), W122 (lower left) and W112 (lower right).

DISTRIBUTION LIST

FFIBM **Dato:** 25 november 2002

RAPPORTTYPE (KRYSS AV)	RAPPORT NR.	REFERANSE	RAPPORTENS DATO
X RAPP ☐ NOTAT ☐ RR	2002/04480	FFIBM/786/115	25 november 2002
RAPPORTENS BESKYTTELSESGRAD		ANTALL EKS UTSTEDT	ANTALL SIDER
Unclassified		30	47
RAPPORTENS TITTEL		FORFATTER(E)	
MATCHED-FIELD LOCALIZATION OF EXPLOSIVE SOURCES IN THE BARENTS SEA USING A HORIZONTAL ARRAY		TOLLEFSEN Dag	
FORDELING GODKJENT AV FORSKNINGSSJEF		FORDELING GODKJENT AV AVDELINGSSJEF:	
J K Johnsen		Jan Ivar Botnan	

EKSTERN FORDELING

ANTALL	EKS NR	TIL
1		FO/E
3		v/ Rådgiver A Berg
1		UVB skvadron 1
1		v/ OK Yngve Skoglund
1		NTNU
		v/ Professor Jens M Hovem
		O. S. Bragstads pl. 2B
		7491 Trondheim
1		Applied Research Laboratories
		v/ Dr David P. Knobles
		The University of Texas at Austin
		PO Box 8029
		Austin, TX 78713-8029, USA
1		School of Earth and Ocean Sciences
		v/ Professor N R Chapman
		University of Victoria
		Box 3055 STN CSC
		Victoria, BC V8W 3P6, Canada

INTERN FORDELING

ANTALL	EKS NR	TIL
14		FFI-Bibl
1		Adm direktør/stabssjef
1		FFIE
1		FFISYS
1		FFIBM
1		FFIN
1		Avd ktr FFIBM/Horten
1		Forfattereksemplar(er)
		ELEKTRONISK FORDELING:
		J K Johnsen (JKJ)
		E J Eidem (EJE)
		T Jenserud (TJE)
		C E Solberg (CES)
		T Svolsbru (TSU)
		K A Søstrand (KAS)
		T Torgersen (TTO)
		FFI-veven

FFI-K1 Retningslinjer for fordeling og forsendelse er gitt i Oraklet, Bind I, Bestemmelser om publikasjoner for Forsvarets forskningsinstitutt, pkt 2 og 5. Benytt ny side om nødvendig.